AD-A141 473 ACTIVE AND PASSIVE REMOTE SENSING OF ICE(U) 1/1
MASSACHUSETTS INST OF TECH CAMBRIDGE RESEARCH LAB OF
ELECTRONICS J A KONG APR 84 N00014-83-K-0258

UNCLASSIFIED F/G 12/1 NL

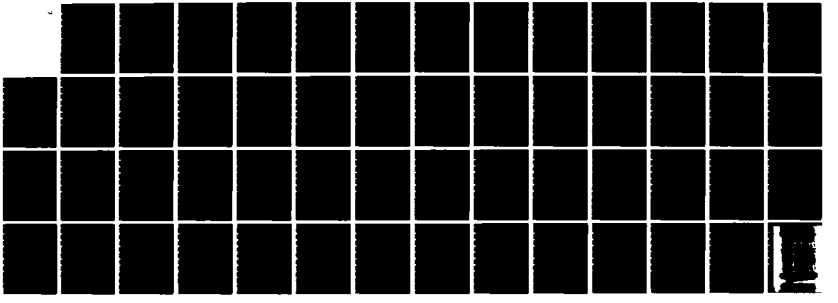

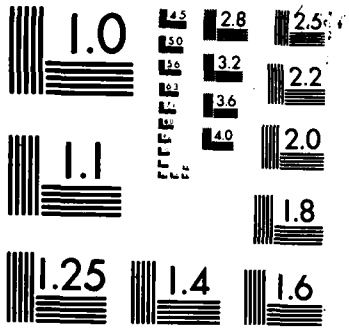

MICROCOPY RESOLUTION TEST CHART
NATIONAL BUREAU OF STANDARDS 1963-A

AD-A141 473

ACTIVE AND PASSIVE REMOTE SENSING OF ICE

Department of the Navy
Office of Naval Research
Contract N00014-83-K-0258

SEMI-ANNUAL REPORT

covering the period

August 1, 1983 - January 31, 1984

prepared by

J. A. Kong

April 1984

Massachusetts Institute of Technology
Research Laboratory of Electronics
Cambridge, Massachusetts 02139

DTIC FILE COPY

2 4 1984
A

This document has been approved for public release and sale; its distribution is unlimited.

84 05 11 012

ACTIVE AND PASSIVE REMOTE SENSING OF ICE

Principal Investigator: Jin Au Kong

SEMI-ANNUAL PROGRESS REPORT

This is a report on the progress that has been made in ~~the~~ study of active and passive remote sensing of ice under the sponsorship of ONR Contract N00014-83-K-0258 during the period of August 1, 1983 - January 31, 1984. During this period ~~we have~~ the investigators (1) derived the backscattering coefficients for a two-layer anisotropic random medium; (2) calculated the emissivities from a two-layer anisotropic random medium ; and (3) participated in the microwave sea ice measurement program at the Cold Regions Research and Engineering Laboratory (CRREL).

A two-layer anisotropic random medium model has been developed to study the active remote sensing of sea and lake ice. The dyadic Green's function for a two-layer anisotropic medium is used in conjunction with the first-order Born approximation to calculate the backscattering coefficients. The random permittivity fluctuation is also assumed to be anisotropic and characterized by the correlation functions which are related to the shape of the fluctuation structure. It is shown that strong cross-polarization occurs in the single scattering process and is indispensable in the interpretation of radar measurements of sea ice at different frequencies, polarization and viewing angles. The theoretical model is also shown to correspond to the ellipsoidal discrete scatterer model, which enables us to determine the relationships

between the cross-correlation and autocorrelation functions. A manuscript has been prepared for submission to a journal for publication [Appendix].

The emissivity of a two-layer anisotropic random medium has been calculated using the dyadic Green's function for a two-layer anisotropic medium and the first-order Born approximation. The emissivity is calculated by obtaining coherent and incoherent reflectivities and by making use of the relationship $e = 1 - r$. The incoherent reflectivity is obtained by integrating over the upper hemisphere the bistatic scattering coefficients obtained under the Born approximation. The theoretical results have been used to interpret the passive microwave remote sensing data from vegetation canopy which also show strong anisotropic dependencies. A manuscript is being prepared to document the theory and the theoretical calculations.

We have participated in the winter microwave remote sensing measurements at CRREL. Several trips were made to the experimental site at CRREL in order to assist and participate in the experimental efforts. Our involvement in the experimental efforts has provided us with valuable insights in the development of theoretical models and data interpretation. We are currently waiting for the calibrated and reduced data in order to start the interpretation of the experimental data with our theoretical models.

Publications Sponsored by ONR

A. Refereed Journal Articles

1. J. K. Lee and J. A. Kong, "Dyadic Green's functions for layered anisotropic medium," Electromagnetics, accepted for publication.

2. J. K. Lee and J. A. Kong, "Active microwave remote sensing of layered anisotropic random medium," to be published.

B. Conference Articles

3. L. Tsang and J. A. Kong, "Scattering of electromagnetic waves from a half-space of densely distributed dielectric scatterers," IEEE/APS Symposium and URSI Meeting, Houston, Texas, May 23-26, 1983.

4. L. Tsang and J. A. Kong, "Theory of microwave remote sensing of dense medium," IEEE/GRS Symposium and URSI Meeting, San Francisco, September 1983.

5. Y. Q. Jin and J. A. Kong, "Wave scattering by a bounded layer of random discrete scatterers," URSI Symposium, Boulder, Colorado, January 11-14, 1984.

6. J. K. Lee and J. A. Kong, "Active and passive microwave remote sensing of layered anisotropic random medium," URSI Symposium, Boston, Mass., June 25-28, 1984.

C. Technical Reports

7. R. T. Shin and J. A. Kong, "Emissivity of a two-layer random medium with anisotropic correlation function," Technical Report No. EWT-RS-41-8303, MIT, 1983.

APPENDIX

ACTIVE MICROWAVE REMOTE SENISNG OF LAYERED ANISOTROPIC RANDOM MEDIUM

Jay Kyoon Lee and Jin Au Kong

Department of Electrical Engineering and
Computer Science and
Research Laboratory of Electronics
Massachusetts Institute of Technology
Cambridge, MA 02139

Abstract

A two-layer anisotropic random medium model has been developed to study the active remote sensing of earth terrain. The dyadic Green's function for a two-layer anisotropic medium is developed and used in conjunction with the first order Born approximation to calculate the backscattering coefficients. It is shown that strong cross polarization occurs in the single scattering process and is indispensable in the interpretation of radar measurements of sea ice at different frequencies, polarization, and viewing angles. The effects of anisotropy on angle responses of backscattreing coefficients are also illustrated.

* This work was supported by the ONR Contract N00014-83-K-0258, the NASA Contract NAG5-270 and the NSF Grant ECS82-03390.

1. Introduction

In the active microwave remote sensing of earth terrain, the random medium model has been used to account for the volume scattering effects of the terrain media such as snow, ice, and vegetation. The problem of scattering by a half space random medium as well as a layered medium has been studied in recent years [1-7]. However, these works assume an isotropic constitutive relation whereas the actual medium may be anisotropic in nature. An example is the dielectric behavior of sea ice. Due to the development of brine inclusions inside the ice crystal, it has been found that the dielectric loss of sea ice is greater when the electric field is parallel to the brine inclusions, as compared to when the field is perpendicular to them [8-9], implying an electrical anisotropy. It has been also observed that the c-axis of the crystal structure of sea ice has a preferred azimuthal orientation [10-14]. The radar backscattering coefficients for sea ice [15-16] also strongly suggests a theoretical model with an anisotropic permittivity tensor. Besides these observations, there are many other experimental data which assert the anisotropic dielectric behavior of sea ice [17-21]. The cross-polarized backscattering coefficients have been calculated with the Born approximation [22] or the bilocal approximation [23] to second order with the isotropic random medium model in layered structures. However, the large cross-polarization components as measured in sea ice strongly suggest that the effect is a first order contribution.

In this paper we study the problem of active remote sensing with a two-layer anisotropic random medium model. The dyadic Green's function for a two-layer anisotropic medium is first obtained and approximated in the far field. The random permittivity fluctuation is then characterized by three correlation functions: (i) the autocorrelation between azimuthal fluctuations at two different spatial points, (ii) the autocorrelation between vertical fluctuations at two points, and (iii) the cross-correlation between azimuthal and vertical fluctuations at two points. With the information about the shape of the fluctuation structure known, the third is related to the first two. The first order backscattering coefficients are calculated with the Born approximation. The results are examined and interpreted, emphasizing the effect of anisotropy of the random permittivity on the backscattering coefficients including cross-polarization, as a function of frequency, incidence angle, incidence azimuthal angle, and tilted angle of optic axis. The theoretical model is shown to correspond to the ellipsoidal discrete scatterer model, which also enables us to determine the relationships between the cross-correlation and autocorrelation functions. Finally the theoretical results are applied to the interpretation of experimental data obtained from sea ice measurements.

2. Formulation of the Problem

Consider an electromagnetic plane wave with linearly polarized time-harmonic field

$$\bar{E}_{0i}(\bar{r},t) = \bar{E}_{0i}e^{i(\bar{k}_{oi}\cdot\bar{r}-\omega t)} \tag{2.1}$$

incident upon a layer of an anisotropic random medium with a permittivity tensor

$$\bar{\bar{\epsilon}}_1(\bar{r}) = <\bar{\bar{\epsilon}}_1(r)> + \bar{\bar{\epsilon}}_{1f}(\bar{r}) \tag{2.2}$$

where $<\bar{\bar{\epsilon}}_1(\bar{r})>$ is the mean part and $\bar{\bar{\epsilon}}_{1f}(\bar{r})$ represents the randomly fluctuating part [Fig. 1]. For the statistically homogeneous medium, $<\bar{\bar{\epsilon}}_1(\bar{r})>$ will be a constant independent of position. $\bar{\bar{\epsilon}}_{1f}(\bar{r})$ is a centered random function of position and its ensemble average, $<\bar{\bar{\epsilon}}_{1f}(\bar{r})>$, is zero. It is assumed that the amplitude of $\bar{\bar{\epsilon}}_{1f}(\bar{r})$ is small compared to $<\bar{\bar{\epsilon}}_1(\bar{r})>$. In general, both $<\bar{\bar{\epsilon}}_1(\bar{r})>$ and $\bar{\bar{\epsilon}}_{1f}(\bar{r})$ are taken to be uniaxial with the optic axis tilted off the z-axis by some angle. For example, in the case of sea ice, the brine inclusions inside ice crystal are elongated and have preferred directions which are tilted from the vertical axis [19]. The optic axes of $<\bar{\bar{\epsilon}}_1(\bar{r})>$ and $\bar{\bar{\epsilon}}_{1f}(\bar{r})$ are rotated by ψ and ψ_f, respectively, from the z-axis around the x-axis so that they are in the yz-plane as shown in Fig. 2.

By the rotaton of coordinate axes, the mean permittivity tensors $<\bar{\bar{\epsilon}}_1^o(\bar{r}')>$ and $<\bar{\bar{\epsilon}}_1(\bar{r})>$, before and after tilting, respectively, are obtained as follows.

$$<\bar{\bar{\epsilon}}_1^o(\bar{r}')> = \begin{bmatrix} \epsilon_1 & 0 & 0 \\ 0 & \epsilon_1 & 0 \\ 0 & 0 & \epsilon_{1z} \end{bmatrix} \tag{2.3}$$

$$<\bar{\bar{\epsilon}}_1(\bar{r})> = \begin{bmatrix} \epsilon_{11} & 0 & 0 \\ 0 & \epsilon_{22} & \epsilon_{23} \\ 0 & \epsilon_{32} & \epsilon_{33} \end{bmatrix} \equiv \bar{\bar{\epsilon}}_{1m} \tag{2.4}$$

where

$$\begin{aligned} \epsilon_{11} &= \epsilon_1, \quad \epsilon_{22} = \epsilon_1\cos^2\psi + \epsilon_{1z}\sin^2\psi \\ \epsilon_{23} &= \epsilon_{32} = (\epsilon_{1z} - \epsilon_1)\cos\psi\sin\psi \\ \epsilon_{33} &= \epsilon_1\sin^2\psi + \epsilon_{1z}\cos^2\psi \end{aligned} \tag{2.5}$$

Similarly, the permittivity fluctuation tensors can be written as

$$\bar{\bar{\epsilon}}_{1f}^o(\bar{r}') = \begin{bmatrix} \epsilon_{1f}(\bar{r}') & 0 & 0 \\ 0 & \epsilon_{1f}(\bar{r}') & 0 \\ 0 & 0 & \epsilon_{1zf}(\bar{r}') \end{bmatrix} \tag{2.6}$$

$$\bar{\bar{\epsilon}}_{1f}(\bar{r}) = \begin{bmatrix} \epsilon_{11f}(r) & 0 & 0 \\ 0 & \epsilon_{22f}(\bar{r}) & \epsilon_{23f}(r) \\ 0 & \epsilon_{32f}(\bar{r}) & \epsilon_{33f}(\bar{r}) \end{bmatrix} \tag{2.7}$$

where

$$\epsilon_{11f}(\bar{r}) = \epsilon_{1f}, \quad \epsilon_{22f}(\bar{r}) = \epsilon_{1f}\cos^2\psi_f + \epsilon_{1zf}\sin^2\psi_f,$$
$$\epsilon_{23f}(\bar{r}) = \epsilon_{32f}(\bar{r}) = (\epsilon_{1zf} - \epsilon_{1f})\cos\psi_f \sin\psi_f, \tag{2.8}$$
$$\epsilon_{33f}(\bar{r}) = \epsilon_{1f}\sin^2\psi_f + \epsilon_{1zf}\cos^2\psi_f.$$

The layer of random medium has boundaries at $z = 0$ and $z = -d$. The upper region is free space and isotropic with permittivity ϵ_o and the lower region is homogeneous and isotropic with permittivity ϵ_2. All three regions are assumed to have the same permeability μ.

The total electric field in region 0 which is the sum of incident and scattered fields satisfies the following homogeneous vector wave equation

$$\nabla \times \nabla \times \bar{E}_0(\bar{r}) - k_o^2\, \bar{E}_0(\bar{r}) = 0, \qquad z \geq 0 \tag{2.9}$$

where $k_o^2 = w^2\mu\epsilon_o$. The electric field in region 1 satisfies

$$\nabla \times \nabla \times \bar{E}_1(\bar{r}) - w^2\mu\bar{\bar{\epsilon}}_1(\bar{r}) \cdot \bar{E}_1(\bar{r}) = 0, \qquad -d \leq z \leq 0 \tag{2.10}$$

i.e.

$$\nabla \times \nabla \times \bar{E}_1(\bar{r}) - w^2\mu\bar{\bar{\epsilon}}_{1m} \cdot \bar{E}_1(\bar{r}) = \bar{\bar{Q}}(\bar{r}) \cdot \bar{E}_1(\bar{r}), \qquad -d \leq z \leq 0 \tag{2.11}$$

where $\bar{\bar{Q}}(\bar{r}) = w^2\mu\bar{\bar{\epsilon}}_{1f}(\bar{r})$ is treated as an effective source distribution.

We can express the formal solutions of (2.9) and (2.11) for the electric fields in both regions in terms of dyadic Green's functions.

$$\bar{E}_0(\bar{r}) = \bar{E}_0^{(0)}(\bar{r}) + \int_{V_1} d^3\bar{r}_1\, \bar{\bar{G}}_{01}(\bar{r}, \bar{r}_1) \cdot \bar{\bar{Q}}(\bar{r}_1) \cdot \bar{E}_1(\bar{r}_1) \tag{2.12}$$

$$\bar{E}_1(\bar{r}) = \bar{E}_1^{(0)}(\bar{r}) + \int_{V_1} d^3\bar{r}_1\, \bar{\bar{G}}_{11}(\bar{r}, \bar{r}_1) \cdot \bar{\bar{Q}}(\bar{r}_1) \cdot \bar{E}_1(\bar{r}_1) \tag{2.13}$$

where the integrations extend over region 1 occupied by the random medium.

The superscript zero in $\bar{E}_0^{(0)}(\bar{r})$ and $\bar{E}_1^{(0)}(\bar{r})$ refers to the unperturbed solutions in the absence of the random fluctuation part. We will use the parenthesized superscripts (1), (2), (3), etc. to denote higher-order terms. The dyadic Green's functions, $\bar{\bar{G}}_{01}(\bar{r}, \bar{r}_1)$ and $\bar{\bar{G}}_{11}(\bar{r}, \bar{r}_1)$, satisfy

$$\nabla \times \nabla \times \bar{\bar{G}}_{01}(\bar{r}, \bar{r}_1) - w^2\mu\epsilon_o\bar{\bar{G}}_{01}(\bar{r}, \bar{r}_1) = 0, \qquad z \geq 0 \tag{2.14}$$

$$\nabla \times \nabla \times \overline{\overline{G}}_{11}(\bar{r}, \bar{r}_1) - \omega^2 \mu_{1m} \cdot \overline{\overline{G}}_{11}(\bar{r}, \bar{r}_1) = I\delta(\bar{r} - \bar{r}_1), \qquad -d \le z \le 0 \tag{2.15}$$

with the appropriate boundary conditions at $z = 0$ and $z = -d$ and radiation conditions at $z = \pm\infty$ for the electric fields. Here the first and second subscripts refer to the regions of the field and source points, respectively.

We can obtain the solutions to (2.12) and (2.13) by iteration. Repeating the substitution of (2.13) into (2.12) we find the solution for the total electric field in region 0, in the form of the infinite Neumann series [24] .

$$\overline{E}_0(\bar{r}) = \overline{E}_0^{(0)}(\bar{r}) + \sum_{n=1}^{\infty} \overline{E}_0^{(n)}(\bar{r}) \tag{2.16}$$

where

$$\overline{E}_0^{(1)}(\bar{r}) = \int_{V_1} d^3\bar{r}_1 \, \overline{\overline{G}}_{01}(\bar{r}, \bar{r}_1) \cdot \overline{\overline{Q}}(\bar{r}_1) \cdot \overline{E}_1^{(0)}(\bar{r}_1) \tag{2.17}$$

$$\overline{E}_0^{(2)}(\bar{r}) = \int_{V_1} d^3\bar{r}_1 d^3\bar{r}_2 \left[\overline{\overline{G}}_{01}(\bar{r}, \bar{r}_1) \cdot \overline{\overline{Q}}(\bar{r}_1)\right] \cdot \left[\overline{\overline{G}}_{11}(\bar{r}_1, \bar{r}_2) \cdot \overline{\overline{Q}}(\bar{r}_2)\right] \cdot \overline{E}_1^{(0)}(\bar{r}_2) \tag{2.18}$$

$$\begin{aligned} \overline{E}_0^{(n)}(\bar{r}) = \int_{V_1} d^3\bar{r}_1 d^3\bar{r}_2 \cdots d^3\bar{r}_n &\left[\overline{\overline{G}}_{01}(\bar{r}, \bar{r}_1) \cdot \overline{\overline{Q}}(\bar{r}_1)\right] \cdot \left[\overline{\overline{G}}_{11}(\bar{r}_1, \bar{r}_2) \cdot \overline{\overline{Q}}(\bar{r}_2)\right] \\ &\cdots \left[\overline{\overline{G}}_{11}(\bar{r}_{n-1}, \bar{r}_n) \cdot \overline{\overline{Q}}(\bar{r}_n)\right] \cdot \overline{E}_1^{(0)}(\bar{r}_n) \end{aligned} \tag{2.19}$$

$\overline{E}_0^{(1)}(\bar{r})$ is the first-order scattered field and the rest is the higher-order scattered fields. Physically, $\overline{E}_0^{(1)}(\bar{r})$ accounts for the single scattering, $\overline{E}_0^{(2)}(\bar{r})$ accounts for the double scattering, and so on. If the scattering is weak, we would expect that the series in (2.16) will converge rapidly. Then the first term in the infinite series expansion will provide a good approximation to the scattered field.

$$\overline{E}_0(\bar{r}) \equiv \overline{E}_0^{(0)}(\bar{r}) + \overline{E}_0^{s}(\bar{r}) \approx \overline{E}_0^{(0)}(\bar{r}) + \overline{E}_0^{(1)}(\bar{r}). \tag{2.20}$$

Now we impose the so-called first-order Born approximation by replacing $\overline{E}_1(\bar{r}_1)$ in (2.12) by $\overline{E}_1^{(0)}(\bar{r}_1)$, as shown in (2.20). In order to find the quantity of physical interest we form the absolute square of $\overline{E}_0(\bar{r})$ and take its ensemble average. Then the mean intensity of the electric fild in region 0 will become

$$< |\overline{E}_0(\bar{r})|^2 > \approx |\overline{E}_0^{(0)}(\bar{r})|^2 + < |\overline{E}_0^{(1)}(\bar{r})|^2 > \tag{2.21}$$

where we used $Re < \overline{E}_0^{(0)}(\bar{r}) \cdot \overline{E}_0^{(1)}(\bar{r})^* >= Re\overline{E}_0^{(0)}(\bar{r}) \cdot < \overline{E}_0^{(1)}(\bar{r})^* >= 0$ because $< \overline{\overline{Q}}(\bar{r}_1) >= 0$. Therefore, the first-order scattered intensity in region 0 is given by

$$\begin{aligned} < |\overline{E}_0^{s}(\bar{r})|^2 > \approx \; & < |\overline{E}_0^{(1)}(\bar{r})|^2 > = \int\int_V d^3\bar{r}_1 d^3\bar{r}_2 \\ & \left\langle \left[\overline{\overline{G}}_{01}(\bar{r}, \bar{r}_1) \cdot \overline{\overline{Q}}(\bar{r}_1) \cdot \overline{E}_1^{(0)}(\bar{r}_1)\right] \cdot \left[\overline{\overline{G}}_{01}(\bar{r}, \bar{r}_2) \cdot \overline{\overline{Q}}(\bar{r}_2) \cdot \overline{E}_1^{(0)}(\bar{r}_2)\right]^* \right\rangle \end{aligned} \tag{2.22}$$

Expressing the dyadic Green's function, the fluctuation tensor, and the unperturbed electric field in terms of components in Cartesian coordinates, the scattered field intensity becomes

$$< |\overline{E}_0^s(\bar{r})|^2 >= \sum_{i,j,k,l,m=1}^{3} \int\int_V d^3\bar{r}_1 d^3\bar{r}_2 [G_{ij}(\bar{r},\bar{r}_1)E_k(\bar{r}_1)] \\ [G_{il}(\bar{r},\bar{r}_2)E_m(\bar{r}_2)]^* \langle Q_{jk}(\bar{r}_1)Q_{lm}^*(\bar{r}_2)\rangle \tag{2.23}$$

3. Dyadic Green's Function and Unperturbed Electric Field

In order to proceed with the calculation of the scattered intensity, we first have to find the dyadic Green's function (DGF) for a two-layered anisotropic (tilted-uniaxial) medium, $\overline{\overline{G}}_{01}(\bar{r},\bar{r}')$, with the observation point in region 0 and the source point in region 1. We take the resultant expression for the DGF, $\overline{\overline{G}}_{10}(\bar{r},\bar{r}')$, with the observation point in region 1 and the source point in region 0, which are derived in Ref. [25] and apply the following symmetrical property of DGF [26]

$$\overline{\overline{G}}_{01}(\bar{r},\bar{r}') = \overline{\overline{G}}_{10}^{T}(\bar{r}',\bar{r}) \tag{1}$$

where the superscript T denotes the transpose of the matrix or dyadic. Exchanging the arguments, $\bar{r}$ and $\bar{r}'$, in (31b) of Ref. [25] and taking its transpose, we obtain $\overline{\overline{G}}_{01}$ as follows.

$$\begin{aligned}\overline{\overline{G}}_{01}(\bar{r},\bar{r}') &= \frac{i}{8\pi^2}\int\int_{-\infty}^{\infty} dk_x dk_y \frac{1}{k_{oz}} e^{i\bar{k}_{\rho}\cdot\bar{r}}\Big\{\hat{h}_o(k_{oz})\Big[A_{oH}\hat{o}(k_{1z}^{o})e^{-i\bar{k}_1^{o}\cdot\bar{r}'} \\ &+ B_{oH}\hat{o}(-k_{1z}^{o})e^{-i\bar{\kappa}_1^{o}\cdot\bar{r}'} + A_{eH}\hat{c}(k_{1z}^{eu})e^{i\bar{k}_1^{e}\cdot\bar{r}'} + B_{eH}\hat{e}(k_{1z}^{ed})e^{-i\bar{\kappa}_1^{e}\cdot\bar{r}'}\Big] \\ &+ \hat{v}_o(k_{oz})[A_{oV}\hat{o}(k_{1z}^{o})e^{-i\bar{k}_1^{o}\cdot\bar{r}'} + B_{oV}\hat{(}-k_{1z}^{o})e^{-i\bar{\kappa}_1^{o}\cdot\bar{r}'} + A_{eV}\hat{c}(k_{1z}^{eu})e^{-i\bar{k}_1^{e}\cdot\bar{r}'} \\ &+ B_{eV}\hat{e}(k_{1z}^{ed})e^{-i\bar{\kappa}_1^{e}\cdot\bar{r}'}\Big]\Big\}\end{aligned} \tag{3.2}$$

where

$$\hat{h}_o(k_{oz}) = \frac{1}{k_\rho}\hat{z}\times\bar{k}_o \tag{3.3a}$$

$$\hat{v}_o(k_{oz}) = \frac{1}{k_o}\hat{h}_o(k_{oz})\times\bar{k}_o \tag{3.3b}$$

$$\hat{o}(k_{1z}^{o}) = \frac{\hat{z}'\times\bar{k}_1^{o}}{|\hat{z}'\times\bar{k}_1^{o}|} \tag{3.3c}$$

$$\hat{o}(-k_{1z}^{o}) = \frac{\hat{z}'\times\bar{\kappa}_1^{o}}{|\hat{z}'\times\bar{\kappa}_1^{o}|} \tag{3.3d}$$

$$\hat{e}(k_{1z}^{eu}) = \frac{\hat{o}(k_{1z}^{eu})\times\bar{k}_{1u}}{|\bar{k}_{1u}|} \tag{3.3e}$$

$$\hat{c}(k_{1z}^{ed}) = \frac{\hat{o}(k_{1z}^{ed})\times\bar{\kappa}_{1u}}{|\bar{\kappa}_{1u}|} \tag{3.3f}$$

$$\hat{o}(k_{1z}^{eu}) = \frac{\hat{z}'\times\bar{k}_1^{e}}{|\hat{z}'\times\bar{k}_1^{e}|} \tag{3.3g}$$

$$\hat{o}(k_{1z}^{ed}) = \frac{\hat{z}' \times \bar{\kappa}_1^e}{|\hat{z}' \times \bar{\kappa}_1^e|} \tag{3.3h}$$

$$\bar{k}_o = \bar{k}_\rho + k_{oz}\hat{z} \tag{3.3i}$$

$$\bar{k}_1^o = \bar{k}_\rho + k_{1z}^o \hat{z} \tag{3.3j}$$

$$\bar{\kappa}_1^o = \bar{k}_\rho - k_{1z}^o \hat{z} \tag{3.3k}$$

$$\bar{k}_1^e = \bar{k}_\rho + k_{1z}^{eu}\hat{z} \tag{3.3l}$$

$$\bar{\kappa}_1^e = \bar{k}_\rho + k_{1z}^{ed}\hat{z} \tag{3.3m}$$

$$\bar{k}_{1u} = \bar{\bar{\epsilon}}_{1m} \cdot \bar{k}_1^e \tag{3.3n}$$

$$\bar{\kappa}_{1u} = \bar{\bar{\epsilon}}_{1m} \cdot \bar{\kappa}_1^e \tag{3.3o}$$

$$\bar{k}_\rho = k_x\hat{x} + k_y\hat{y} \tag{3.3p}$$

$$\hat{z}' = \hat{y}\sin\psi + \hat{z}\cos\psi \tag{3.3q}$$

$$k_{iz} = \sqrt{k_i^2 - k_\rho^2}, \qquad i = 0, 2 \tag{3.3r}$$

$$k_{1z}^o = \sqrt{k_1^2 - k_\rho^2} \tag{3.3s}$$

$$\begin{bmatrix} k_{1z}^{eu} \\ k_{1z}^{ed} \end{bmatrix} = -\frac{\epsilon_{23}}{\epsilon_{33}}k_y \pm \frac{1}{\epsilon_{33}}\left[k_1^2\epsilon_{1z}\epsilon_{33} - \epsilon_1\epsilon_{33}k_x^2 - \epsilon_1\epsilon_{1z}k_y^2\right]^{1/2} \tag{3.3t}$$

$$k_i = \omega\sqrt{\mu\epsilon_i}, \qquad i = 0, 1, 2. \tag{3.3u}$$

$$k_\rho = \sqrt{k_x^2 + k_y^2} \tag{3.3v}$$

We notice that $\hat{o}(\pm k_{1z}^o)$ is a unit vector in the direction of an electric field for an ordinary wave and $\hat{e}(k_{1z}^{eu})$ or $\hat{e}(k_{1z}^{ed})$ is one for an extraordinary wave (upward or downward propagating). The coefficients for the upward or downward propagating waves, A's and B's are expressed in terms of the half-space reflection and transmission coefficients as follows.

$$A_{oH} = A_{Ho}(k_x \to -k_x, \quad k_y \to -k_y) \tag{3.4a}$$

$$B_{oH} = B_{Ho}(k_x \to -k_x, \quad k_y \to -k_y) \tag{3.4b}$$

$$A_{eH} = -A_{He}(k_x \to -k_x, \quad k_y \to -k_y) \tag{3.4c}$$

$$B_{eH} = -B_{He}(k_x \to -k_x, \quad k_y \to -k_y) \tag{3.4d}$$

$$A_{oV} = -A_{Vo}(k_x \to -k_x, \quad k_y \to -k_y) \tag{3.4e}$$

$$B_{oV} = -B_{Vo}(k_x \to -k_x, \quad k_y \to -k_y) \tag{3.4f}$$

$$A_{eV} = A_{Ve}(k_x \to -k_x, \quad k_y \to -k_y) \tag{3.1g}$$

$$B_{eV} = B_{Ve}(k_x \to -k_x, \quad k_y \to -k_y) \tag{3.1h}$$

and

$$A_{\beta o}(k_x, k_y) = X_{\beta o} L_1 + X_{\beta e} L_2 \tag{3.5a}$$

$$A_{\beta e}(k_x, k_y) = X_{\beta o} M_2 + X_{\beta e} M_1 \tag{3.5b}$$

$$B_{\beta\gamma}(k_x, k_y) = X_{\beta o}(L_1 o_\gamma + M_2 e_\gamma) + X_{\beta e}(L_2 o_\gamma + M_1 e_\gamma) \tag{3.5c}$$

where

$$\beta = H \quad \text{or} \quad V,$$

$$\gamma = o \quad \text{or} \quad e,$$

and

$$L_1 = \frac{1 - S_{ee}}{D} \tag{3.6a}$$

$$L_2 = \frac{S_{eo}}{D} \tag{3.6b}$$

$$M_1 = \frac{1 - S_{oo}}{D} \tag{3.6c}$$

$$M_2 = \frac{S_{oe}}{D} \tag{3.6d}$$

$$S_{oo} = o_o R_{oo} + o_e R_{eo} \tag{3.6e}$$

$$S_{oe} = o_o R_{oe} + o_e R_{ee} \tag{3.6f}$$

$$S_{eo} = e_o R_{oo} + e_e R_{eo} \tag{3.6g}$$

$$S_{ee} = e_o R_{oe} + e_e R_{ee} \tag{3.6h}$$

$$D = (1 - S_{oo})(1 - S_{ee}) - S_{oe} S_{eo} \tag{3.6i}$$

$$\begin{bmatrix} o_o & e_o \\ o_e & e_e \end{bmatrix} = \begin{bmatrix} e^{ik_{1z}^{o} d} R_{12oo} e^{ik_{1z}^{o} d} & e^{-ik_{1z}^{ed} d} R_{12eo} e^{ik_{1z}^{o} d} \\ e^{ik_{1z}^{o} d} R_{12oe} e^{ik_{1z}^{eu} d} & e^{-ik_{1z}^{ed} d} R_{12ee} e^{ik_{1z}^{eu} d} \end{bmatrix} \tag{3.6j}$$

$$\begin{aligned} X_{Ho} = {} & \frac{g_d}{D_e} \frac{2}{(k_{oz} + k_{1z}^{o})} \frac{k_{oz}}{k_\rho} \{ k_\rho^2 (k_1^2 k_{oz} - k_o^2 k_{1z}^{ed}) \cos\psi \\ & + k_y (k_o^2 k_{1z}^{o2} - k_1^2 k_{oz} k_{1z}^{ed}) \sin\psi \} \end{aligned} \tag{3.7a}$$

$$X_{He} = -\frac{U_d}{D_e} \frac{2k_{oz}}{k_\rho} k_x (k_\rho^2 + k_{oz} k_{1z}^{o}) \sin\psi \tag{3.7b}$$

$$X_{Vo} = \frac{g_d}{D_e} \frac{2k_o k_{oz} k_1^2 k_x}{k_\rho} \frac{k_{oz} - k_{1z}^{ed}}{k_{oz} + k_{1z}^{o}} \sin\psi \tag{3.7c}$$

$$X_{Ve} = \frac{U_d}{D_e}\frac{2k_o}{k_\rho}(k_{oz}k_\rho^2\cos\psi + k_y k_{oz}k_{1z}^o\sin\psi) \tag{3.7d}$$

$$R_{oo} = \frac{g_d}{g_u}\frac{E_e}{D_e}\frac{k_{1z}^o - k_{oz}}{k_{1z}^o + k_{oz}} \tag{3.8a}$$

$$R_{oe} = \frac{U_d}{g_u}\frac{1}{D_e}2k_x k_{1z}^o(k_{1z}^o - k_{oz})(k_y\sin\psi - k_{oz}\cos\psi)\sin\psi \tag{3.8b}$$

$$R_{eo} = \frac{g_d}{U_u}\frac{1}{D_e}k_1^2 k_x(k_{1z}^{ed} - k_{1z}^{eu})(k_{1z}^o - k_{oz})(k_y\sin\psi + k_{oz}\cos\psi)\sin\psi \tag{3.8c}$$

$$R_{ee} = -\frac{U_d}{U_u}\frac{I_e}{D_e} \tag{3.8d}$$

$$R_{12oo} = \frac{g_u}{g_d}\frac{G_e}{F_e}\frac{k_{1z}^o - k_{2z}}{k_{1z}^o + k_{2z}} \tag{3.9a}$$

$$R_{12oe} = \frac{U_u}{g_d}\frac{1}{F_e}2k_x k_{1z}^o(k_{2z} - k_{1z}^o)(k_y\sin\psi + k_{2z}\cos\psi)\sin\psi \tag{3.9b}$$

$$R_{12eo} = \frac{g_u}{U_d}\frac{1}{F_e}k_1^2 k_x(k_{1z}^{eu} - k_{1z}^{ed})(k_{1z}^o - k_{2z})(k_y\sin\psi - k_{2z}\cos\psi)\sin\psi \tag{3.9c}$$

$$R_{12ee} = \frac{-U_u}{U_d}\frac{H_e}{F_e} \tag{3.9d}$$

$$g_d = \left\{k_x^2 + (k_y\cos\psi + k_{1z}^o\sin\psi)^2\right\}^{1/2} \tag{3.10a}$$

$$g_u = \left\{k_x^2 + (k_y\cos\psi - k_{1z}^o\sin\psi)^2\right\}^{1/2} \tag{3.10b}$$

$$U_d = \left\{\frac{\epsilon_1}{\epsilon_1 - \epsilon_{1z}}\left(k_x^2 + k_y^2 + k_{1z}^{ed^2} - \omega^2\mu\epsilon_1\right)\left[k_x^2 + k_y^2 + k_{1z}^{ed_2} - \omega^2\mu(\epsilon_1 + \epsilon_{1z})\right]\right\}^{1/2} \tag{3.10c}$$

$$U_u = \left\{\frac{\epsilon_1}{\epsilon_1 - \epsilon_{1z}}(k_x^2 + k_y^2 + k_{1z}^{eu_2} - \omega^2\mu\epsilon_1)\left[k_x^2 + k_y^2 + k_{1z}^{eu_2} - \omega^2\mu(\epsilon_1 + \epsilon_{1z})\right]\right\}^{1/2} \tag{3.10d}$$

$$\begin{aligned} D_e &= \cos^2\psi k_\rho^2(k_1^2 k_{oz} - k_o^2 k_{1z}^{ed}) + \sin^2\psi\{k_1^2(k_{oz} - k_{1z}^{ed})(k_x^2 + k_{oz}k_{1z}^o) \\ &\quad + k_y^2 k_{1z}^o(k_1^2 - k_o^2)\} + \cos\psi\sin\psi k_y(k_{1z}^o + k_{oz})(k_{1z}^o - k_{1z}^{ed})(k_\rho^2 + k_{1z}^o k_{oz}) \end{aligned} \tag{3.10e}$$

$$\begin{aligned} E_e &= \cos^2\psi k_\rho^2(k_1^2 k_{oz} - k_o^2 k_{1z}^{ed}) + \sin^2\psi\{k_1^2(k_{oz} - k_{1z}^{ed})(k_x^2 - k_{oz}k_{1z}^o) \\ &\quad - k_y^2 k_{1z}^o(k_1^2 - k_o^2)\} + \cos\psi\sin\psi k_y(k_{1z}^o - k_{oz})(k_{1z}^o + k_{1z}^{ed})(k_\rho^2 - k_{oz}k_{1z}^o) \end{aligned} \tag{3.10f}$$

$$\begin{aligned} I_e &= \cos^2\psi k_\rho^2(k_1^2 k_{oz} - k_o^2 k_{1z}^{eu}) + \sin^2\psi\{k_1^2(k_{oz} - k_{1z}^{eu})(k_x^2 + k_{oz}k_{1z}^o) \\ &\quad + k_y^2 k_{1z}^o(k_1^2 - k_o^2)\} + \cos\psi\sin\psi k_y(k_{1z}^o + k_{oz})(k_{1z}^o - k_{1z}^{eu})(k_\rho^2 + k_{oz}k_{1z}^o) \end{aligned} \tag{3.10g}$$

$$\begin{aligned} F_e &= \cos^2\psi k_\rho^2(k_1^2 k_{2z} + k_2^2 k_{1z}^{eu}) + \sin^2\psi\{k_1^2(k_{2z} + k_{1z}^{eu})(k_x^2 + k_{2z}k_{1z}^o) \\ &\quad + k_y^2 k_{1z}^o(k_1^2 - k_2^2)\} - \cos\psi\sin\psi k_y(k_{1z}^o + k_{2z})(k_{1z}^o + k_{1z}^{eu})(k_\rho^2 + k_{1z}^o k_{2z}) \end{aligned} \tag{3.10h}$$

$$\begin{aligned} G_e &= \cos^2\psi k_\rho^2(k_1^2 k_{2z} + k_2^2 k_{1z}^{eu}) + \sin^2\psi\{k_1^2(k_{2z} + k_{1z}^{eu})(k_x^2 - k_{2z}k_{1z}^o) \\ &\quad - k_y^2 k_{1z}^o(k_1^2 - k_2^2)\} + \cos\psi\sin\psi k_y(k_{2z} - k_{1z}^o)(k_{1z}^o - k_{1z}^{eu})(k_\rho^2 - k_{2z}k_{1z}^o) \end{aligned} \tag{3.10i}$$

$$\begin{aligned} \Pi_e &= \cos^2\psi k_\rho^2(k_1^2 k_{2z} + k_2^2 k_{1z}^{ed}) + \sin^2\psi\{k_1^2(k_{2z} + k_{1z}^{ed})(k_z^2 + k_{2z}k_{1z}^o) \\ &\quad + k_y^2 k_{1z}^o(k_1^2 - k_2^2)\} - \cos\psi\sin\psi k_y(k_{1z}^o + k_{2z})(k_{1z}^o + k_{1z}^{ed})(k_\rho^2 + k_{1z}^o k_{2z}) \end{aligned} \tag{3.10j}$$

Under the far-field approximation, the integral for $\overline{\overline{G}}_{01}(\bar{r},\bar{r}')$ in (3.2) is evaluated with the method of steepest descent [27,28] as $r \to \infty$. The results are

$$\overline{\overline{G}}_{01}(\bar{r},\bar{r}') = \frac{e^{ik_o r}}{4\pi r} e^{-i\bar{k}_\rho\cdot\bar{\rho}'}\,\overline{\overline{g}}(\bar{k}_\rho, z') \tag{3.11a}$$

where

$$\begin{aligned} \overline{\overline{g}}(\bar{k}_\rho, z') &= \hat{h}_o(k_{oz})\Big[A_{oH}\hat{o}(k_{1z}^o e^{-ik_{1z}^o z'} + B_{oH}\hat{o}(-k_{1z}^o)e^{ik_{1z}^o z'} \\ &\quad + A_{eH}\hat{e}(k_{1z}^{eu})e^{-ik_{1z}^{eu}z'} + B_{eH}\hat{e}(k_{1z}^{ed})e^{-ik_{1z}^{ed}z'}\Big] \\ &\quad + \hat{v}_o(k_{oz})\Big[A_{oV}\hat{o}(k_{1z}^o)e^{-ik_{1z}^o z'} + B_{oV}\hat{o}(-k_{1z}^o)e^{ik_{1z}^o z'} \\ &\quad + A_{eV}\hat{e}(k_{1z}^{eu})e^{-ik_{1z}^{eu}z'} + B_{eV}\hat{e}(k_{1z}^{ed})e^{-ik_{1z}^{ed}z'}\Big] \end{aligned} \tag{3.11b}$$

and all the coefficients and the vectors are defined in (3.3)-(3.10) with

$$k_x = k_o \sin\theta_s \cos\phi_s \tag{3.12a}$$

$$k_y = k_o \sin\theta_s \sin\phi_s \tag{3.12b}$$

and (θ_s, ϕ_s) are the observation angles in the scattered direction.

Given the wave incident form region 0 with TE or TM polarization and the amplitude E_{0i}, the unperturbed electric fields in region 1, $\overline{E}_1^{(0)}(\bar{r})$, are obtained in a similar manner as $\overline{\overline{G}}_{10}(\bar{r},\bar{r}')$ was.

$$\begin{aligned} \overline{E}_1^{(0)}(\bar{r})^{TE} &= E_{0i}\Big\{A_{Hei}\hat{o}(-k_{1zi}^o)e^{-ik_{1zi}^o z} + B_{Hei}\hat{o}(k_{1zi}^o)e^{ik_{1zi}^o z} \\ &\quad + A_{Hei}\hat{e}(k_{1zi}^{eu})e^{ik_{1zi}^{eu}z} + B_{Hei}\hat{e}(k_{1zi}^{ed})e^{ik_{1zi}^{ed}z}\Big\}e^{i\bar{k}_{xi}\cdot\bar{\rho}} \end{aligned} \tag{3.13a}$$

$$\begin{aligned} \overline{E}_1^{(0)}(\bar{r})^{TM} &= E_{0i}\Big\{A_{Vei}\hat{o}(-k_{1zi}^o)e^{-ik_{1zi}^o z} + B_{Vei}\hat{o}(k_{1zi}^o)e^{ik_{1zi}^o z} \\ &\quad + A_{Vei}\hat{e}(k_{1zi}^{eu})e^{ik_{1zi}^{eu}z} + B_{Vei}\hat{e}(k_{1zi}^{ed})e^{ik_{1zi}^{ed}z}\Big\}e^{i\bar{k}_{xi}\cdot\bar{\rho}} \end{aligned} \tag{3.13b}$$

where

$$A_{\beta\gamma i} = A_{\beta\gamma}(k_x = k_{xi},\ k_y = k_{yi}) \tag{3.14a}$$

$$B_{\beta\gamma i} = B_{\beta\gamma}(k_x = k_{xi},\ k_y = k_{yi}) \tag{3.14b}$$

$$\beta = H \quad \text{or} \quad V$$

$$\gamma = o \quad \text{or} \quad e$$

$$\bar{k}_{\rho i} = k_{xi}\hat{x} + k_{yi}\hat{y} \tag{3.15a}$$

$$k_{1zi}^{o} = \sqrt{k_1^2 - k_{\rho i}^2} \tag{3.15b}$$

$$\begin{Bmatrix} k_{1zi}^{eu} \\ k_{1zi}^{ed} \end{Bmatrix} = -\frac{\epsilon_{23}}{\epsilon_{33}} k_{yi} \pm \frac{1}{\epsilon_{33}} [k_1^2 \epsilon_{1x}\epsilon_{33} - \epsilon_1 \epsilon_{33} k_{xi}^2 - \epsilon_1 \epsilon_{1x} k_{yi}^2]^{1/2} \tag{3.15c}$$

$$k_{\rho i} = \sqrt{k_{xi}^2 + k_{yi}^2} \tag{3.15d}$$

$$k_{xi} = k_o \sin\theta_{0i} \cos\phi_{0i} \tag{3.15e}$$

$$k_{yi} = k_o \sin\theta_{0i} \sin\phi_{0i} \tag{3.15f}$$

and (θ_{0i}, ϕ_{0i}) are the observation angles in the incident direction.

4. Correlation Function of Permittivity Fluctuation

The permittivity fluctuation tensor $\overline{\overline{Q}}(\bar{r}) = \omega^2\mu\bar{\bar{\epsilon}}_{1f}(\bar{r})$ of the random medium is assumed to be not only uniaxial but also tilted by some angle ψ_f as was discussed in Section 2. The fluctuation tensors $\overline{\overline{Q}}_o(\bar{r}')$ and $\overline{\overline{Q}}(\bar{r})$, before and after tilting, respectively, are given by

$$\overline{\overline{Q}}_o(\bar{r}') = \begin{bmatrix} Q(\bar{r}') & 0 & 0 \\ 0 & Q(\bar{r}') & 0 \\ 0 & 0 & Q_z(\bar{r}') \end{bmatrix} \tag{4.1a}$$

$$\overline{\overline{Q}}(\bar{r}) = \begin{bmatrix} Q_{11}(\bar{r}) & 0 & 0 \\ 0 & Q_{22}(\bar{r}) & Q_{23}(\bar{r}) \\ 0 & Q_{32}(\bar{r}) & Q_{33}(\bar{r}) \end{bmatrix} \tag{4.1b}$$

where

$$\begin{aligned} Q_{11} &= Q, \qquad Q_{22} = Q\cos^2\psi_f + Q_z\sin^2\psi_f \\ Q_{23} &= Q_{32} = (Q_z - Q)\cos\psi_f\sin\psi_f \\ Q_{33} &= Q\sin^2\psi_f + Q_z\cos^2\psi_f \end{aligned} \tag{4.2}$$

following the equations (2.6)-(2.8).

In order to calculate the scattered intensity in (2.23) we have to determine the correlation function $< Q_{jk}(\bar{r}_1)Q^*_{lm}(\bar{r}_2) >$. Because the random medium is assumed to be statistically homogeneous, the correlation function depends only upon the separation of two spatial points $\bar{r}_1$ and $\bar{r}_2$[29],

$$< Q_{jk}(\bar{r}_1)Q^*_{lm}(\bar{r}_2) > \equiv C_{jklm}(\bar{r}_1 - \bar{r}_2) \tag{4.3}$$

Next we express $C_{jklm}(\bar{r}_1 - \bar{r}_2)$ in terms of its own Fourier transform

$$C_{jklm}(\bar{r}_1 - \bar{r}_2) = k_1'^4 \int d^3\bar{\beta}\Phi_{jklm}(\bar{\beta})e^{-i\bar{\beta}\cdot(\bar{r}_1 - \bar{r}_2)} \tag{4.4}$$

where $k_1' = Re(k_1)$ and $\Phi_{jklm}(\bar{\beta})$ is the power spectral density of the correlation function.

We define three correlation functions and their spectral densities :

$$< Q(\bar{r}_1)Q^*(\bar{r}_2) > \equiv C_1(\bar{r}_1 - \bar{r}_2) = k_1'^4 \int d^3\bar{\beta}\ \Phi_1(\bar{\beta})\, e^{-i\bar{\beta}\cdot(\bar{r}_1 - \bar{r}_2)} \tag{4.5a}$$

$$< Q_z(\bar{r}_1)Q_z^*(\bar{r}_2) > \equiv C_2(\bar{r}_1 - \bar{r}_2) = k_1'^4 \int d^3\bar{\beta}\ \Phi_2(\bar{\beta})\, e^{-i\bar{\beta}\cdot(\bar{r}_1 - \bar{r}_2)} \tag{4.5b}$$

$$< Q(\bar{r}_1)Q_z^*(\bar{r}_2) > \equiv C_3(\bar{r}_1 - \bar{r}_2) = k_1'^4 \int d^3\bar{\beta}\ \Phi_3(\bar{\beta})\, e^{-i\bar{\beta}\cdot(\bar{r}_1 - \bar{r}_2)} \tag{4.5c}$$

where $C_1(\bar{r}_1 - \bar{r}_2)$ and $C_2(\bar{r}_1 - \bar{r}_2)$ are the autocorrelation functions of the random physical quanties $Q(\bar{r})$ and $Q_z(\bar{r})$, respectively, and $C_3(\bar{r}_1 - \bar{r}_2)$ is the crosscorrelation function of

the above two random quanties at two different spatial points. $C_3(r_1 - r_2)$ is, in general, independent of $C_1(r_1 - r_2)$ and $C_2(r_1 - r_2)$, but given some information about the shape of fluctuation it will depend on C_1 and C_2. We will specify C_3 in terms of C_1 and C_2 comparing with the result of the ellipsoidal discrete scatterer model in Section 6. Now we can express all spectral densities $\Phi_{jklm}(\bar{\beta})$ in (4.4) in terms of $\Phi_1(\bar{\beta})$, $\Phi_2(\bar{\beta})$, and $\Phi_3(\bar{\beta})$ defined in (4.5) using (4.2).

$$
\begin{aligned}
\Phi_{1111} &= \Phi_1 \\
\Phi_{1122} &= \Phi_{2211} = \Phi_1 \cos^2\psi_f + \Phi_3 \sin^2\psi_f \\
\Phi_{1133} &= \Phi_{3311} = \Phi_1 \sin^2\psi_f + \Phi_3 \cos^2\psi_f \\
\Phi_{2222} &= \Phi_1 \cos^4\psi_f + \Phi_2 \sin^4\psi_f + 2\Phi_3 \cos^2\psi_f \sin^2\psi_f \\
\Phi_{2233} &= \Phi_{3322} = (\Phi_1 + \Phi_2)\sin^2\psi_f \cos^2\psi_f + \Phi_3(\sin^4\psi_f + \cos^4\psi_f) \\
\Phi_{3333} &= \Phi_1 \sin^4\psi_f + \Phi_2 \cos^4\psi_f + 2\Phi_3 \cos^2\psi_f \sin^2\psi_f
\end{aligned}
\tag{4.6}
$$

$$
\begin{aligned}
\Phi_{1123} &= \Phi_{1132} = \Phi_{2311} = \Phi_{3211} = (\Phi_3 - \Phi_1)\sin\psi_f \cos\psi_f \\
\Phi_{2223} &= \Phi_{2232} = \Phi_{2322} = \Phi_{3222} \\
&= [(\Phi_3 - \Phi_1)\cos^2\psi_f + (\Phi_2 - \Phi_3)\sin^2\psi_f]\sin\psi_f \cos\psi_f \\
\Phi_{3323} &= \Phi_{3332} = \Phi_{2333} = \Phi_{3233} \\
&= [(\Phi_3 - \Phi_1)\sin^2\psi_f + (\Phi_2 - \Phi_3)\cos^2\psi_f]\sin\psi_f \cos\psi_f \\
\Phi_{2323} &= \Phi_{2332} = \Phi_{3223} = \Phi_{3232} = (\Phi_1 + \Phi_2 - 2\Phi_3)\sin^2\psi_f \cos^2\psi_f
\end{aligned}
$$

We characterize the correlation function by considering two quantities, variance and correlation length. Let's consider the correlation function of the fluctuation which is Gaussian in lateral direction and exponential in vertical direction.

$$
C_1(\bar{r}_1 - \bar{r}_2) = \delta_1 k_1'^4 \exp\left[-\frac{|\bar{\rho}_1 - \bar{\rho}_2|^2}{l_\rho^2}\right]\exp\left[-\frac{|z_1 - z_2|}{l_z}\right] \tag{4.7}
$$

$$
C_2(\bar{r}_1 - \bar{r}_2) = \delta_2 k_1'^4 \exp\left[-\frac{|\bar{\rho}_1 - \bar{\rho}_2|^2}{l_\rho^2}\right]\exp\left[-\frac{|z_1 - z_2|}{l_z}\right] \tag{4.8}
$$

where δ_1 and δ_2 are the normalized variances of the lateral and vertical components of the permittivity fluctuation tensor, respectively, and l_ρ and l_z are the correlation lengths in lateral and vertical directions, respectively.

Here we took the same correlation lengths for two different correlation functions in (4.7) and (4.8). It is physically reasonable to assume the correlation lengths to be the same no matter what the physical quantity is. In other words, the correlation length depends only on the randomness of the medium and it does not depend on the physical quantity (Q and Q_z). But it may differ from direction to direction so that we have two correlation lengths in two different directions, lateral and vertical.

On the other hand, the variance which is the strength of fluctuation can depend on the physical quantity. $\delta_1 \neq \delta_2$ describes the anisotropy of the permittivity fluctuation of the random medium in our model and leads to the first order depolarized backscattering.

5. Backscattering Coefficients

Substituting the resultant expressions for the unperturbed electric field $\overline{E}_1^{(0)}(r)$ in (3.13), the far-field approximated dyadic Green's function $\overline{\overline{G}}_{01}(\bar{r}, \bar{r}_1)$ in (3.11), and the correlation function defined by (4.3), into (2.23), we obtain

$$< |\overline{E}_0^s(\bar{r})|^2 >= \frac{|E_{0i}|^2}{(4\pi r)^2} \int\int d^2\bar{\rho}_1 d^2\bar{\rho}_2 \, e^{-i(\bar{k}_\rho - \bar{k}_{\rho i})\cdot\bar{\rho}_1} \, e^{i(\bar{k}_\rho - \bar{k}_{\rho i})\cdot\bar{\rho}_2}$$
$$\sum_{\substack{i,j,k \\ l,m}}^{3} \int\int_{-d}^{0} dz_1 dz_2 \, g_{ij}(\bar{k}_\rho, z_1) F_k(\bar{k}_{\rho i}, z_1) g_{il}^*(\bar{k}_\rho, z_2) F_m^*(\bar{k}_{\rho i}, z_2) C_{jklm}(\bar{r}_1 - \bar{r}_2) \tag{5.1}$$

where

$$\overline{E}_1^{(0)}(\bar{r}_l) = E_{0i} e^{i\bar{k}_{\rho i}\cdot\bar{\rho}_l} \overline{F}(\bar{k}_{\rho i}, z_l), \quad l = 1, 2 \tag{5.2a}$$
$$F_k(\bar{k}_{\rho i}, z_l) = \hat{x}_k \cdot \overline{F}(\bar{k}_{\rho i}, z_l), \qquad k = 1, 2, 3 \tag{5.2b}$$
$$g_{ij}(\bar{k}_\rho, z_l) = \hat{x}_i \cdot \overline{\overline{g}}(\bar{k}_\rho, z_l) \cdot \hat{x}_j, \quad i, j = 1, 2, 3 \tag{5.2c}$$
$$\hat{x}_1 = \hat{x}, \; \hat{x}_2 = \hat{y}, \; \hat{x}_3 = \hat{z}. \tag{5.2d}$$

Making use of (4.4),

$$< |\overline{E}_0^s(\bar{r})|^2 >= \frac{|E_{0i}|^2 k_1'^4}{(4\pi r)^2} \int_{-\infty}^{\infty} d^3\bar{\beta} \int\int d^2\bar{\rho}_1 d^2\bar{\rho}_2 \, e^{i(\bar{k}_{\rho i} - \bar{k}_\rho - \bar{\beta}_\perp)\cdot\bar{\rho}_1} \, e^{-i(\bar{k}_{\rho i} - \bar{k}_\rho - \bar{\beta}_\perp)\cdot\bar{\rho}_2}$$
$$\sum_{\substack{i,j,k \\ l,m}} \int\int_{-d}^{0} dz_1 dz_2 \, g_{ij}(z_1) F_k(z_1) g_{il}^*(z_2) F_m^*(z_2) \, \Phi_{jklm}(\bar{\beta}) \, e^{-i\beta_z(z_1 - z_2)} \tag{5.3}$$

where $\bar{\beta}_\perp = \beta_x\hat{x} + \beta_y\hat{y}$ and $\Phi_{jklm}(\bar{\beta})$ is given by (4.6). After the $\bar{\rho}_1$ -integration,

$$< |\overline{E}_0^s(\bar{r})|^2 >= \frac{|E_{0i}|^2 k_1'^4}{(4\pi r)^2} \int d^2\bar{\rho}_2 \int_{-\infty}^{\infty} d^2\bar{\beta}_\perp (2\pi)^2 \delta(\bar{k}_{\rho i} - \bar{k}_\rho - \bar{\beta}_\perp) e^{-i(\bar{k}_{\rho i} - \bar{k}_\rho - \bar{\beta}_\perp)\cdot\bar{\rho}_2}$$
$$\sum_{\substack{i,j,k \\ l,m}} \int_{-\infty}^{\infty} d\beta_z \int\int_{-d}^{0} dz_1 dz_2 g_{ij}(z_1) F_k(z_1) g_{il}^*(z_2) F_m^*(z_2) \Phi_{jklm}(\bar{\beta}_\perp, \beta_z) e^{-i\beta_z(z_1 - z_2)} \tag{5.4}$$

The delta function enables the $\bar{\beta}_\perp$ -integration to be performed and then the $\bar{\rho}_2$ -integration will give the illuminated area A ;

$$< |\overline{E}_0^s(\bar{r})|^2 >= \frac{A|E_{0i}|^2 k_1'^4}{4r^2} \sum_{\substack{i,j,k \\ l,m}} \int_{-\infty}^{\infty} d\beta_z \int\int_{-d}^{0} dz_1 dz_2 \, g_{ij}(z_1) F_k(z_1) g_{il}^*(z_2) F_m^*(z_2)$$
$$\Phi_{jklm}(\bar{\beta}_\perp = \bar{k}_{\rho i} - \bar{k}_\rho, \beta_z) \, e^{-i\beta_z(z_1 - z_2)} \tag{5.5}$$

For the case of backscattered direction where $\bar{k}_\rho = -\bar{k}_{\rho s}$ and $k_{1z} = k_{1zs}$, we will have to evaluate the integral of the following form.

$$I = \int_{-\infty}^{\infty} d\beta_z \int_{-d}^{0} dz_1 \int_{-d}^{0} dz_2 e^{\imath(k''_{1zs}+k''^{q}_{1zs})z_1} e^{-\imath(k''^{*s}_{1zs}+k''^{*t}_{1zs})z_2} \Phi(\bar{\beta}_\perp = 2\bar{k}_{\rho s}, \beta_z) e^{-\imath\beta_z(z_1-z_2)} \tag{5.6}$$

$$= \int_{-\infty}^{\infty} d\beta_z \Phi(\beta_2) \frac{[1-e^{-\imath d(k''^{p}_{1zs}+k''^{q}_{1zs}-\beta_z)}][1-e^{\imath d(k''^{*s}_{1zs}+k''^{*t}_{1zs}-\beta_z)}]}{(k''^{p}_{1zi}+k''^{q}_{1zi}-\beta_z)(k''^{*s}_{1zi}+k''^{*t}_{1zi}-\beta_z)} \tag{5.7}$$

where

$$\left\{ \begin{matrix} p\,, & q \\ s\,, & t \end{matrix} \right\} = \begin{cases} ou\,; & k_{1zi} = k^{o}_{1zi} \\ od\,; & k_{1zi} = -k^{o}_{1zi} \\ eu\,; & k_{1zi} = k^{eu}_{1zi} \\ ed\,; & k_{1zi} = k^{ed}_{1zi} \end{cases}$$

The β_z-integration will be performed term by term using the contour integration of the residue calculus and we pick up the dominant pole-contributions under some reasonable approximations. The value of integration is significant only when $p = s, q = t$ or $p = t, q = s$ and the result is the following.

$$I \approx \begin{cases} 2\pi\Phi(\beta_z = k'^{p}_{1zi} + k'^{q}_{1zi}) \frac{e^{2(k''^{p}_{1zs}+k''^{q}_{1zs})d}-1}{2(k''^{p}_{1zs}+k''^{q}_{1zs})} & \text{for } p=s,\ q=t \text{ or } p=t,\ q=s \quad (5.8) \\ 2\pi\Phi(\beta_z = 0)d, & \text{only for } k^{p}_{1zi} = -k^{q}_{1zi} \quad (5.9) \end{cases}$$

where $'$ denotes the real part and $''$ denotes the imaginary part of that quantity.

Now given the spectral density of the correlation function, we can determine the first order scattered intensity by a two-layered anisotropic random medium.

The assumptions we made in evaluating the above integrals are given below.

(i)

$$k''^{o}_{1zi} \ll k'^{o}_{1zi}, \qquad k''^{e}_{1zi} \ll k'^{e}_{1zi} \tag{5.10a}$$

(The medium is slightly lossy.)

(ii)

$$d \gg l_z \tag{5.10b}$$

(The random medium layer of interest contains many scattering inhomogeneities along the vertical direction.)

(iii)

$$k'^{o}_{1zi} d > 1, \qquad k'^{e}_{1zi} d > 1 \tag{5.10c}$$

(The scattering layer contains many wavelengths.)

All the above assumptions are reasonable in the microwave remote sensing of the earth terrain. For example, in the case of sea ice, a typical correlation length is on the order of millimeters while typical layer thickness is on the order of meters [30]. Moreover, we assumed that $\Phi(\bar{\beta})$ vanishes everywhere on the hemi-circle at infinity. This assumption of course is not satisfied by all correlation functions. However, it does include many physically interesting correlation functions.

In addition, because of the tilted uniaxial fluctuation, we need to have the coordinate transformations in order to get correct expressions for $\Phi(\bar{\beta})$ which we use in (5.3) — (5.5). Since the fluctuation is uniaxial in $x'y'z'$ -coordinate as shown in Fig. 2, the correlation function $C(\bar{r}_1 - \bar{r}_2)$ is expressed as

$$C(\bar{R}') = k_1'^4 \int d^3\bar{\alpha}\, \hat{\Phi}(\bar{\alpha}) \exp\left[-i\bar{\alpha}\cdot\bar{R}'\right] \tag{5.11}$$

where

$$\bar{R}' = \bar{r}_1' - \bar{r}_2' \equiv \hat{x}x' + \hat{y}y' + \hat{z}z' \tag{5.12a}$$

$$\bar{\alpha} = \hat{x}\alpha_x + \hat{y}\alpha_y + \hat{z}\alpha_z \tag{5.12b}$$

For example, the correlation function which is Gaussian laterally and exponential vertically

$$C(\bar{R}') = \delta k_1'^4 \exp\left[-\left|\frac{\bar{\rho}'}{l_\rho}\right|^2\right] \exp\left[-\left|\frac{z'}{l_z}\right|\right] \tag{5.13}$$

has the Fourier transform

$$\hat{\Phi}(\bar{\alpha}) = \frac{\delta l_z l_\rho^2}{4\pi^2(1+\alpha_z^2 l_z^2)} \exp\left[-\frac{\alpha_x^2+\alpha_y^2}{4} l_\rho^2\right] \tag{5.14}$$

We like to transform $C(\bar{R}')$ and $\hat{\Phi}(\bar{\alpha})$ into the form in xyz -coordinate, $C(\bar{R})$ and $\Phi(\bar{\beta})$, so that we can substitute them in (5.3)–(5.5).

$$C(\bar{R}') \equiv C(\bar{R}) = k_1'^4 \int d^3\bar{\beta}\, \Phi(\bar{\beta}) \exp\left[-i\bar{\beta}\cdot\bar{R}\right] \tag{5.15}$$

where

$$\bar{R} = \bar{r}_1 - \bar{r}_2 \equiv \hat{x}x + \hat{y}y + \hat{z}z \tag{5.16a}$$

$$\bar{\beta} = \hat{x}\beta_x + \hat{y}\beta_y + \hat{z}\beta_z \tag{5.16b}$$

Using the coordinate transformations [Fig. 2],

$$\begin{aligned} x' &= x \\ y' &= y\cos\psi - z\sin\psi \\ z' &= y\sin\psi + z\cos\psi \end{aligned} \tag{5.17}$$

we obtain the following relations between $\bar{\alpha}$ and $\bar{\beta}$:

$$\begin{aligned} \alpha_x &= \beta_x \\ \alpha_y &= \beta_y\cos\psi - \beta_z\sin\psi \\ \alpha_z &= \beta_y\sin\psi + \beta_z\cos\psi \end{aligned} \tag{5.18}$$

$$\begin{aligned} \beta_x &= \alpha_x \\ \beta_y &= \alpha_y\cos\psi + \alpha_z\sin\psi \\ \beta_z &= -\alpha_y\sin\psi + \alpha_z\cos\psi \end{aligned} \tag{5.19}$$

Then

$$d\alpha_x d\alpha_y d\alpha_z = d\beta_x J\left(\frac{\alpha_y, \alpha_z}{\beta_y, \beta_z}\right) d\beta_y d\beta_z \tag{5.20}$$

where

$$J\left(\frac{\alpha_y, \alpha_z}{\beta_y, \beta_z}\right) = \begin{vmatrix} \frac{\partial\alpha_y}{\partial\beta_y} & \frac{\partial\alpha_y}{\partial\beta_z} \\ \frac{\partial\alpha_z}{\partial\beta_y} & \frac{\partial\alpha_z}{\partial\beta_z} \end{vmatrix} = 1$$

Using (5.17)–(5.20), from (5.11) and (5.15) we obtain

$$\Phi(\bar{\beta}) = \hat{\Phi}(\alpha_x = \beta_x,\ \alpha_y = \beta_y\cos\psi - \beta_z\sin\psi,\ \alpha_z = \beta_y\sin\psi + \beta_z\cos\psi) \tag{5.21}$$

For the correlation function given by (5.13), we have

$$\Phi(\bar{\beta}) = \frac{\delta l_z l_\rho^2 \exp\left[-\frac{1}{4}\beta_x^2 l_\rho^2\right] \exp\left[-\frac{1}{4}(\beta_y\cos\psi - \beta_z\sin\psi)^2 l_\rho^2\right]}{4\pi^2[1 + (\beta_y\sin\psi + \beta_z\cos\psi)^2 l_z^2]} \tag{5.22}$$

Making use of (5.8) and (5.9) for evaluation of the integral in (5.5) and letting $\theta_s = \theta_{0i}$ and $\phi_s = \pi + \phi_{0i}$ where θ_s and ϕ_s are the observation angles in the scattered direction, we obtain the backscattering coefficients which is defined by Peake [31] as

$$\sigma_{\beta\alpha} \equiv \lim_{\substack{A\to\infty \\ r\to\infty}} \frac{4\pi r^2 < |\bar{E}_0^s(\bar{r})|^2 >_\alpha}{A|\bar{E}_{0i}|_\beta^2}, \qquad \beta, \alpha = H \text{ or } V \tag{5.23}$$

where $|\bar{E}_{0i}|_\beta^2$ is the incident electric field intensity with polarization β, $< |\bar{E}_0^s(\bar{r})|^2 >_\alpha$ is the mean scattered field intensity with polarization α, and β and α can be either horizontal (TE) or vertical (TM) polarization. The final results are the following.

$$\sigma_{\beta\alpha} = 2\pi^2 k_1'^4 \sum_{i=1}^{11} J_i(A's, B's, k_{1z}'s, d, R's) \tag{5.24}$$

where

$$J_1 = |A_{\alpha oi}A_{\beta oi}|^2 \frac{1-e^{-4k''^o_{1zi}d}}{4k''^o_{1zi}} R_A(-k'^o_{1zi}, -k'^o_{1zi}, -2k'^o_{1zi}) \tag{5.25a}$$

$$J_2 = |A_{\alpha oi}B_{\beta oi} + B_{\alpha oi}A_{\beta oi}|^2 d\, R_A(k'^o_{1zi}, -k'^o_{1zi}, 0) \tag{5.25b}$$

$$J_3 = |B_{\alpha oi}B_{\beta oi}|^2 \frac{1-e^{4k''^o_{1zi}d}}{-4k''^o_{1zi}} R_A(k'^o_{1zi}, k'^o_{1zi}, 2k'^o_{1zi}) \tag{5.25c}$$

$$J_4 = |A_{\alpha oi}A_{\beta ei} + A_{\alpha ei}A_{\beta oi}|^2 \frac{1-e^{-2(k''^o_{1zi}-k''^{ed}_{1zi})d}}{2(k''^o_{1zi}-k''^{ed}_{1zi})} R_B(-k'^o_{1zi}, k'^{ed}_{1zi}, -k'^o_{1zi}+k'^{ed}_{1zi}) \tag{5.25d}$$

$$J_5 = |A_{\alpha oi}B_{\beta ei} + B_{\alpha ei}A_{\beta oi}|^2 \frac{1-e^{-2(k''^o_{1zi}-k''^{eu}_{1zi})d}}{2(k''^o_{1zi}-k''^{eu}_{1zi})} R_B(-k'^o_{1zi}, k'^{eu}_{1zi}, -k'^o_{1zi}+k'^{eu}_{1zi}) \tag{5.25e}$$

$$J_6 = |B_{\alpha oi}A_{\beta ei} + A_{\alpha ei}B_{\beta oi}|^2 \frac{1-e^{2(k''^o_{1zi}+k''^{ed}_{1zi})d}}{-2(k''^o_{1zi}+k''^{ed}_{1zi})} R_B(k'^o_{1zi}, k'^{ed}_{1zi}, k'^o_{1zi}+k'^{ed}_{1zi}) \tag{5.25f}$$

$$J_7 = |B_{\alpha oi}B_{\beta ei} + B_{\alpha ei}B_{\beta oi}|^2 \frac{1-e^{2(k''^o_{1zi}+k''^{eu}_{1zi})d}}{-2(k''^o_{1zi}+k''^{eu}_{1zi})} R_B(k'^o_{1zi}, k'^{eu}_{1zi}, k'^o_{1zi}+k'^{eu}_{1zi}) \tag{5.25g}$$

$$J_8 = |A_{\alpha ei}A_{\beta ei}|^2 \frac{1-e^{4k''^{ed}_{1zi}d}}{-4k''^{ed}_{1zi}} R_C(k'^{ed}_{1zi}, k'^{ed}_{1zi}, 2k'^{ed}_{1zi}) \tag{5.25h}$$

$$J_9 = |A_{\alpha ei}B_{\beta ei} + B_{\alpha ei}A_{\beta ei}|^2 \frac{1-e^{2(k''^{ed}_{1zi}+k''^{eu}_{1zi})d}}{-2(k''^{ed}_{1zi}+k''^{eu}_{1zi})} R_C(k'^{ed}_{1zi}, k'^{eu}_{1zi}, k'^{ed}_{1zi}+k'^{eu}_{1zi}) \tag{5.25i}$$

$$J_{10} = |B_{\alpha ei}B_{\beta ei}|^2 \frac{1-e^{4k''^{eu}_{1zi}d}}{-4k''^{eu}_{1zi}} R_C(k'^{eu}_{1zi}, k'^{eu}_{1zi}, 2k'^{eu}_{1zi}) \tag{5.25j}$$

$$J_{11} = \Delta \cdot 2Re(A_{vei}B_{Hoi}B^*_{vei}A^*_{Hoi})d\, R'_B \tag{5.25k}$$

$$\begin{aligned} R_A(X,Y,\beta_z) &= \frac{1}{[g(X)g(Y)]^2}\{C^2_{11A}\Phi_{1111}(\beta_z) + 2C_{11A}C_{22A}\Phi_{1122}(\beta_z) + C^2_{22A}\Phi_{2222}(\beta_z) \\ &+ 2C_{11A}C_{33A}\Phi_{1133}(\beta_z) + 2C_{22A}C_{33A}\Phi_{2233}(\beta_z) + C^2_{33A}\Phi_{3333}(\beta_z) \\ &+ 2C_{11A}C_{23A}\Phi_{1123}(\beta_z) + 2C_{22A}C_{23A}\Phi_{2223}(\beta_z) \\ &+ 2C_{33A}C_{23A}\Phi_{2333}(\beta_z) + C^2_{23A}\Phi_{2323}(\beta_z)\} \end{aligned} \tag{5.26a}$$

$$\begin{aligned} R_B(X,Y,\beta_z) &= \{C^2_{11B}\Phi_{1111}(\beta_z) + 2C_{11B}C_{22B}\Phi_{1122}(\beta_z) + C^2_{22B}\Phi_{2222}(\beta_z) \\ &+ 2C_{11B}C_{33B}\Phi_{1133}(\beta_z) + 2C_{22B}C_{33B}\Phi_{2233}(\beta_z) + C^2_{33B}\Phi_{3333}(\beta_z) \\ &+ 2C_{11B}C_{23B}\Phi_{1123}(\beta_z) + 2C_{22B}C_{23B}\Phi_{2223}(\beta_z) \\ &+ 2C_{33B}C_{23B}\Phi_{2333}(\beta_z) + C^2_{23B}\Phi_{2323}(\beta_z)\} \end{aligned} \tag{5.26b}$$

$$\begin{aligned} R_C(X,Y,\beta_z) &= \{C^2_{11C}\Phi_{1111}(\beta_z) + 2C_{11C}C_{22C}\Phi_{1122}(\beta_z) + C^2_{22C}\Phi_{2222}(\beta_z) \\ &+ 2C_{11C}C_{33C}\Phi_{1133}(\beta_z) + 2C_{22C}C_{33C}\Phi_{2233}(\beta_z) + C^2_{33C}\Phi_{3333}(\beta_z) \\ &+ 2C_{11C}C_{23C}\Phi_{1123}(\beta_z) + 2C_{22C}C_{23C}\Phi_{2223}(\beta_z) \\ &+ 2C_{33C}C_{23C}\Phi_{2333}(\beta_z) + C^2_{23C}\Phi_{2323}(\beta_z)\} \end{aligned} \tag{5.26c}$$

$$R'_B = \frac{1}{(k_{\rho i}^2 k_1)^2}\{-(k_{xi}k_{yi}k'^{o}_{1zi})^2[\Phi_{1111}(0) + \Phi_{2222}(0) - 2\Phi_{1122}(0)] + (k_{xi}k_{\rho i}^2)^2\Phi_{2323}(0)\} \quad (5.26d)$$

$$g(X) = \{k_{xi}^2 + (k_{yi}\cos\psi - X\sin\psi)^2\}^{1/2} \quad (5.27a)$$

$$U(X) = \left\{\frac{\epsilon_1}{\epsilon_1 - \epsilon_{1z}}(k_{\rho i}^2 + X^2 - \omega^2\mu\epsilon_1)[k_{\rho i}^2 + X^2 - \omega^2\mu(\epsilon_1 + \epsilon_{1z})]\right\}^{1/2} \quad (5.27b)$$

$$C_{11A}(X,Y) = (k_{yi}\cos\psi - X\sin\psi)(k_{yi}\cos\psi - Y\sin\psi) \quad (5.28a)$$

$$C_{22A} = k_{xi}^2\cos^2\psi \quad (5.28b)$$

$$C_{33A} = k_{xi}^2\sin^2\psi \quad (5.28c)$$

$$C_{23A} = -2k_{xi}^2\sin\psi\cos\psi \quad (5.28d)$$

$$C_{11B}(X,Y) = k_{xi}(k_{yi}\cos\psi - X\sin\psi)(k_{yi}\sin\psi + Y\cos\psi) \quad (5.29a)$$

$$C_{22B}(X,Y) = -k_{xi}\cos\psi[k_{yi}(k_{yi}\sin\psi + Y\cos\psi) - k_1^2\sin\psi] \quad (5.29b)$$

$$C_{33B}(X,Y) = k_{xi}\sin\psi[Y(k_{yi}\sin\psi + Y\cos\psi) - k_1^2\cos\psi] \quad (5.29c)$$

$$C_{23B}(X,Y) = k_{xi}[k_{yi}^2\sin^2\psi - Y^2\cos^2\psi + k_1^2\cos 2\psi] \quad (5.29d)$$

$$C_{11C}(X,Y) = k_{xi}^2(k_{yi}\sin\psi + X\cos\psi)(k_{yi}\sin\psi + Y\cos\psi) \quad (5.30a)$$

$$C_{22C}(X,Y) = [k_{yi}(k_{yi}\sin\psi + X\cos\psi) - k_1^2\sin\psi][k_{yi}(k_{yi}\sin\psi + Y\cos\psi) - k_1^2\sin\psi] \quad (5.30b)$$

$$C_{33C}(X,Y) = [X(k_{yi}\sin\psi + X\cos\psi) - k_1^2\cos\psi][Y(k_{yi}\sin\psi + Y\cos\psi) - k_1^2\cos\psi] \quad (5.30c)$$

$$\begin{aligned} C_{23C}(X,Y) &= [k_{yi}(k_{yi}\sin\psi + X\cos\psi) - k_1^2\sin\psi][Y(k_{yi}\sin\psi + Y\cos\psi) - k_1^2\cos\psi] \\ &+ [X(k_{yi}\sin\psi + X\cos\psi) - k_1^2\cos\psi][k_{yi}(k_{yi}\sin\psi + Y\cos\psi) - k_1^2\sin\psi] \end{aligned} \quad (5.30d)$$

$$\Phi_{jklm}(\beta_z) = \Phi_{jklm}(\overline{\beta}_\perp = 2\overline{k}_{\rho i}, \beta_z) \quad (5.31)$$

$$\Delta = \begin{cases} 1, & \text{only for } \sigma_{\beta\alpha} = \sigma_{HV} \text{ or } \sigma_{VH} \text{ when } \psi = 0,\ \epsilon_1 = \epsilon_{1z} \\ 0, & \text{otherwise} \end{cases} \quad (5.32)$$

6. Discussion and Application of the Results

We have obtained the backscattering coefficients for a two-layer anisotropic random medium in (5.24)-(5.32). In the limiting case when both mean and fluctuation are isotropic, i.e. when $\epsilon_{1z} = \epsilon_1, \epsilon_{1zf} = \epsilon_{1f}$, and $\psi = \psi_f = 0$, the results reduce to

$$\sigma_{HH} = \pi^2 k_1''^4 \left| \frac{X_{01i}}{D_{2i}} \right|^4 \left\{ \frac{1 - e^{-4k''_{1zi}d}}{2k''_{1zi}} \left[1 + |R_{12i}|^4 e^{-4k''_{1zi}d} \right] \Phi_1^{(1)} + 8d|R_{12i}|^2 e^{-4k''_{1zi}d} \Phi_1^{(2)} \right\} \tag{6.1a}$$

$$\sigma_{VV} = \pi^2 k_1''^4 \left| \frac{Y_{01i}}{F_{2i}} \right|^4 \frac{k_0^4}{|k_1|^8} \left\{ \frac{1 - e^{-4k''_{1zi}d}}{2k''_{1zi}} \left[1 + |S_{12i}|^4 e^{-4k''_{1zi}d} \right] \left| k_{1zi}^2 + k_0^2 \sin^2 \theta_{0i} \right|^2 \Phi_1^{(1)} + 8d|S_{12i}|^2 e^{-4k''_{1zi}d} \left| k_{1zi}^2 - k_0^2 \sin^2 \theta_{0i} \right|^2 \Phi_1^{(2)} \right\} \tag{6.1b}$$

$$\sigma_{HV} = \sigma_{VH} = 0 \tag{6.1c}$$

These are exactly the same as the results obtained for the case of two-layer isotropic random medium by Zuniga and Kong [6]. As an another limit we let $\psi = 0$ for the case of vertically uniaxial mean and tilted uniaxial fluctuation ($\psi_f \neq 0$). The results check with Lee's [32].

Comparing with the result of the active microwave remote sensing of two-layer homogeneous medium containing ellipsoidal discrete scatterers [33] for the case of prolate spheroid which seems to be similar to our anisotropic continuous random medium model, our result with $\psi = 0$ has one-to-one correspondence with them term by term except the one which comes from the coherent effect between oppositely scattered waves. From the comparison of two results term by term, we get the constraint on the spectral density of $< Q(\bar{r}_1) Q_2^*(\bar{r}_2) >$ in (4.5c):

$$\Phi_3^2(\bar{\beta}) = \Phi_1(\bar{\beta}) \Phi_2(\bar{\beta}). \tag{6.2}$$

Assuming that the three correlation functions in (4.5) have the same statistical behavior, (6.2) leads to

$$\delta_3^2 = \delta_1 \delta_2 \tag{6.3}$$

Therefore, given that the shape of fluctuation is a spheroidal ellipsoid, the cross correlation between Q and Q_2 will be determined by $\Phi_3^2 = \Phi_1 \Phi_2$. We shall use this constraint in assigning statistical parameters in order to get various responses of σ in the following. We shall choose the correlation function to be exponential both laterally and vertically as follows.

$$C_1(\bar{r}_1 - \bar{r}_2) = \delta_1 k_1''^4 exp\left[-\frac{|x_1 - x_2|}{l_\rho} - \frac{|y_1 - y_2|}{l_\rho} - \frac{|z_1 - z_2|}{l_z} \right] \tag{6.4a}$$

$$C_2(\bar{r}_1 - \bar{r}_2) = \delta_2 k_1'^4 \exp\left[-\frac{|x_1 - x_2|}{l_\rho} - \frac{|y_1 - y_2|}{l_\rho} - \frac{|z_1 - z_2|}{l_z}\right] \tag{6.4b}$$

The spectral densities are given as

$$\Phi_j(\bar{\alpha}) = \frac{\delta_j l_\rho^2 l_z}{\pi^2} \frac{1}{(1+\alpha_x^2 l_\rho^2)(1+\alpha_y^2 l_\rho^2)(1+\alpha_z^2 l_z^2)} \qquad j = 1, 2. \tag{6.5}$$

These satisfy the assumptions made in the calculation of σ.

Now we look at various effects of anisotropy of random permittivity. First we see $\sigma_{HV} = \sigma_{VH}$ which agrees with the Lorentz reciprocity theorem since the medium is reciprocal and we consider the scattering in the backscattering direction. The most significant effect is that there is a depolarization in the first-order backscattering. As we see in (6.1c), the first order single scattering with the isotropic random medium model does not induce any depolarization effect in the backscattered direction. Even for the case of uniaxial mean and fluctuation with their optic axes in the z-direction, i.e., when $\epsilon_1 \neq \epsilon_{1z}, \epsilon_{1f} \neq \epsilon_{1zf}$ but $\psi = \psi_f = 0$ (untilted), (5.24) again gives $\sigma_{HV} = \sigma_{VH} = 0$ with some algebraic manipulations. This shows no depolarization. It is physically clear that if the medium is vertically (untilted) uniaxial either in mean or in fluctuation the single scattering in the backscattered direction does not change the polarization of the incident wave. In other words, there is no coupling between two different linear polarizations. However, if either the mean (background) or the fluctuation becomes tilted uniaxial, i.e., $\psi \neq 0$ or $\psi_f \neq 0$, then it gives us nonzero depolarization. We can consider three cases which give the cross polarization effect in the first-order backscattering.

First, $\psi \neq 0$ and $\psi_f = 0$ where the background permittivity is "anisotropic" (tilted uniaxial) and the permittivity fluctuation is isotropic or untilted uniaxial. Then $\sigma_{HV} = \sigma_{VH} \neq 0$. This is because the wave incident with either TE or TM polarization upon an anisotropic background medium produces both the ordindary wave and the extraordinary wave. This is the so-called double refraction.

Second, $\psi_f \neq 0$ and $\psi = 0$ where the fluctuation is anisotropic and the background is isotropic or untilted uniaxial. In this case the wave with one polarization can produce the other polarization, when it is scattered in an anisotropic fluctuation, even in the backscattered direction.

Third, $\psi = \psi_f \neq 0$. It is obvious that when both the background and the fluctuation are anisotropic there would be a strong depolarization effect. It is physically more reasonable to have $\psi = \psi_f$ than $\psi \neq \psi_f$.

It is also to be noted that even if one of three conditions is satisfied, when $\phi_{0i} = \pm 90°$, i.e., when the propagation vector and the optical axis of mean or fluctuation are in the same plane (yz - plane), $\sigma_{HV} = 0$. This is because for this case the electric field is polairzed either perpendicularlly (TE) or parallel (TM) with respect to the plane of incidence so

that the double refraction does not occur and the single scattering does not change the polarization of the incident wave in the backscattered direction.

As an illustration of our theoretical results, the typical responses of σ_{HH}, σ_{VV} and σ_{HV} are shown as a function of frequency at $\theta_{0i} = 30°$ [Fig. 3] and as a function of incidence angle at $f = 10$ GHz [Fig. 4], by choosing the appropriate parameters for $\delta_1, \delta_2, l_\rho$ and l_z which are reasonable numbers in the micowave remote sensing of the earth terrain. We clearly see that we obtain a strong σ_{HV}.

For the backscattering coefficient for the isotropic half-space random medium $(d \to \infty)$ as a function of incidence angle (θ_{0i}), σ_{VV} is always greater than σ_{HH}, because the vertically polarized TM waves are transmitted and backscattered more than horizontally polarized TE waves. In contrast with the isotropic case, the anisotropic half-space random medium gives us the possibility of having $\sigma_{HH} > \sigma_{VV}$ as it will be shown in Figs. 5-10.

First, it is due to an anistropic fluctuation. In Fig. 5, when $\delta_1 > \delta_2$, for large incidence azimuthal angle $\phi_{0i} = 80°$ (near 90°), σ_{HH} is seen to be greater than σ_{VV} especially for small incidence angles θ_{0i}. This is because the strength of fluctuation is stronger in lateral directin (plane perpendicular to the optical axis) compared to that in vertical direction (along the optic axis of fluctuation), in other words, the fluctuation is more correlated in lateral direction. Near $\phi_{0i} = 90°$, the polarizatin of TE wave will be almost in lateral direction with respect to the optical axis of $\overline{\overline{Q}}$. However, for small ϕ_{0i}, it follows the common response, i.e., σ_{VV} is always greater than σ_{HH} over all incidence angles θ_{0i} as shown in Fig. 4.

In Fig. 6, when $\delta_1 < \delta_2$, for small ϕ_{0i} (near 0°), σ_{HH} can be larger than σ_{VV} at small incidence angles so that there is a cross-over between σ_{HH} and σ_{VV} near $\theta_{0i} = 30°$. The reason for this effect is similar as before. TE waves have more components parallel to the optical axis near $\phi_{0i} = 0°$ than at other angles and the fluctuation is more correlated in the direction of optic axis. In contrast, for large ϕ_{0i}, σ_{VV} is always larger than σ_{HH} for all θ_{0i} as shown in Fig. 7. We note that this kind of response can happen when $\psi_f \neq 0$, i.e. for the tilted uniaxial fluctuation.

Second, this phenomena also arises due to an anisotropic background $(\psi \neq 0, \epsilon_1 \neq \epsilon_{1z})$. For example, in Fig. 8, for large ϕ_{0i}, σ_{HH} is greater than σ_{VV} over a wide range of lower θ_{0i} when ϵ''_{1z} deviates largerly from ϵ''_1. See the case of $\epsilon''_1 = 0.01, \epsilon''_{1z} = 0.1$ compared to the case of $\epsilon''_1 = 0.01, \epsilon''_{1z} = 0.02$. This is because TM wave experiences greater absorption than TE waves due to higher loss along the optic axis of the background medium.

The possibility of $\sigma_{HH} > \sigma_{VV}$ can be also seen from the responses of σ as a function of incidence azimuthal angle ϕ_{0i} at a fixed θ_{0i} in Figs. 9-10. When $\delta_1 > \delta_2$ [Fig. 9], σ_{HH} increases and σ_{VV} decreases as ϕ_{0i}, so that $\sigma_{HH} > \sigma_{VV}$ at large ϕ_{0i}. When $\delta_1 < \delta_2$ [Fig. 10], $\sigma_{HH} > \sigma_{VV}$ at small ϕ_{0i}. As a whole, the cross-polarization (σ_{HV}) is

very sensitive to ϕ_{0i}, while the like-polarizations $(\sigma_{HH}, \sigma_{VV})$ are not much affected by changing ϕ_{0i}.

Given the incidence angles, θ_{0i} and ϕ_{0i}, all σ's are affected greatly by changing the tilted angle of optic axis as shown in Figs. 11-12. We observe a lot stronger cross-polarization when $\psi \neq 0$ [Fig. 11] compared to when $\psi = 0$ [Fig. 12]. For some range of ψ, σ_{VH} is as large as σ_{HH} or σ_{VV}. It could be even larger in some cases. From this we observe that the anisotropy of background medium produces more cross-polarization than the anisotropic fluctuation does.

As an application we try to explain the experimental data by matching our theoretical results with experimental data collected from the Arctic sea ice by Onstatt, Moore and Weeks [15].

In Figs. 13-15, we have matched the backscattering data of the thick first-year (TFY) sea ice as a function of an incidence angle at three different frequencies: $f = 9$ GHz [Fig. 13], $f = 13$ GHz [Fig. 14], and $f = 17$ GHz [Fig. 15], simultaneously. The letters H, V, and C represent experimental data for σ_{HH}, σ_{VV} and σ_{HV}, respectively, and the continuous curves represent the theoretical results. In order to match these data we assigned a set of parameters: $l_\rho = 1mm, l_z = 3mm, \delta_1 = 0.1, \delta_2 = 0.8$ with $\phi_{0i} = 75°, \psi = \psi_f = 25°$. The ground truth for ϕ_{0i}, ψ and ψ_f is not known. As seen from the figures, the theoretical results fit with experimental data pretty well except at lower angles. Higher values for σ of experimental data at lower incidence angles compared with the theoretical values are due to the rough surface effect of sea ice surface. Our theory only takes into account the volume scattering and the rough surface scattering effect is not included. Notice that we have chosen $l_z > l_\rho$ and $\delta_2 > \delta_1$. Since the brine inclusions inside an ice crystal look like vertically elongated ellipsoids [19], the vertical correlation length should be greater than the lateral correlation length. The strength of fluctuation in vertical direction is stronger than that in lateral direction, because this quantity determines the magnitude of scattering due to the brine inclusions. We have chosen the different permittivities for sea ice $(\epsilon_1, \epsilon_{1z})$ and sea water (ϵ_2) at different frequencies, following Vant et al. [19] The real part of $\bar{\bar{\epsilon}}_1$ is chosen to be isotropic while the imaginary part is chosen to be anisotropic, following Sackinger and Byrd's report [8].

In Figs. 16-18, we have also matched the backscattering data of the multiyear (MY) sea ice as a function of an incidence angle at three different frequencies: $f = 9$ GHz [Fig. 16], $f = 13$ GHz [Fig. 17], and $f = 17$ GHz [Fig. 18], simultaneously. Another set of parameters are assigned to match data: $l_\rho = 3mm, l_z = 1mm, \delta_1 = 0.1, \delta_2 = 0.3$ with $\phi_{0i} = 75°, \psi = \psi_f = 35°$. The multiyear ice has properties different from those of the first-year ice in that it contains mainly air bubbles and it has much lower salinity [19]. Hence, l_ρ and l_z do not differ much. The dielectric constant and the dielectric loss are expected to be less than those of the thick first-year ice.

7. Conclusions

Introducing the dyadic Green's function formalism and applying the first order Born approixmation, we have solved the problem of electromagnetic wave scattering by a two-layer anisotropic random medium for an application to microwave active remote sensing of earth terrain. With an advantage of wave approach, we obtained the analytic expressions for backscattering coefficients which includes depolarization effect.

There was a significant result in that the anisotropy of mean permittivity or permittivity fluctuation of random medium can lead to nonzero depolarization in the backscattered direction for the first order scattering, in contrast with the isotropic random medium which does not have depolarization in the first order backscattering. Either the mean permittivity or the permittivity fluctuation of the random medium has to be at least uniaxial and tilted with respect to vertical (z) direction in order to obtain the first order depolarized backscattering. The result also shows the possibility of $\sigma_{HH} > \sigma_{VV}$ for an anisotropic random medium even in the case of half-space. This does not occur for an isotropic half-space random medium. As an application to remote sensing, we have matched theoretical results very well with experimental data collected from sea ice.

Since most of the experimental data for backscattering coefficients contains only the incidence angle (θ_{0i}) response, but not the incidence azimuthal angle (ϕ_{0i}) response, it is difficult to take advantage of our anisotropic random medium model at this point. It would be recommended that some experimental data for an azimuthal angle response be collected in order to account for the effect of anisotropy of random permittivity.

References

[1] A. Stogryn, " Electromegnetic scattering by random dielectric constant fluctuations in a bounded medium," *Radio Science*, 9, 509–518, May 1974 .

[2] L. Tsang and J. A. Kong, " Emissivity of half-space random media," *Radio Science*, 11, 593–598, July 1976 .

[3] L. Tsang and J. A. Kong, " Radiative transfer theory for active remote sensing of half-space random media," *Radio Science*, 13, 763–773, Sept.–Oct. 1978 .

[4] A. K. Fung and H. S. Fung, " Application of first-order renormalization method to scattering from a vegetation-like half-space," *IEEE Trans. on Geosci. Electron.*, GE-15, 189–195, Oct. 1977 .

[5] A. K. Fung, " Scattering from a vegetation layer," *IEEE Trans. on Geosci. Electron.*, GE-17, Jan. 1979 .

[6] M. A. Zuniga and J. A. Kong, " Active remote sensing of random media," *J. Appl. Phys.* 51, 74–79, Jan. 1980 .

[7] M. A. Zuniga, T. M. Habashy and J. A. Kong, " Active remote sensing of layered random media," *IEEE Trans. on Geosci. Electron.*, GE-17, 296–302, Oct. 1979 .

[8] W. M. Sackinger and R. C. Byrd, " Reflection of millimeter waves from snow and sea ice," *IAEE Report 7203*, Institute of Arctic Environmental Engineering, Univ. of Alaska, Jan. 1972 .

[9] W. M. Sackinger and R. C. Byrd, " Backscatter of millimeter waves from snow, ice, and sea ice," *IAEE Report 7207*, Institute of Arctic Environmental Engineering, Univ. of Alaska, Dec. 1972 .

[10] K. J. Campbell and A. S. Orange, " The electrical anisotropy of sea ice in the horizontal plane," *J. Geophy. Res.*, 79, 5059–5063, Nov. 1974 .

[11] A. Kovacs and R. M. Morey, " Radar anisotropy of sea ice due to preferred azimuthal orientation of the horizontal c-axes of ice crystals," *J. Geophys. Res.*, 83, 6037–6046, Dec. 1978 .

[12] A. Kovacs and R. M. Morey, " Anisotropic properties of sea ice in the 50- to 150-MHz range," *J. Geophys. Res.*, 84, 5749–5759, Sept. 1979 .

[13] W. F. Weeks and A. J. Gow, " Preferred crystal orientations in the fast ice along the margins of the Arctic ocean," *J. Geophy. Res.*, 83, 5105–5121, Oct. 1978 .

[14] W. F. Weeks and A. J. Gow, " Crystal alignments in the fast ice of Arctic Alaska," *J. Geophy. Res.*, 85, 1137–1146, Feb. 1980 .

[15] R. G. Onstott, R. K. Moore and W. F. Weeks, " Surface-based scatterometer results of Arctic sea ice," *IEEE Trans. on Geosci. Electron.*, GE-17, 78–85, July

1979 .

[16] C. V. Delker, R. G. Onstott and R. K. Moore, " Radar scatterometer measurements of sea ice: the SURSAT experiment," *RSL Technical Report*, RSL TR331-17, Rem. Sens. Lab., Univ. of Kansas, Lawrence, KS, Aug. 1980 .

[17] P. Hoekstra and P. Cappillino, " Dielectric properties of sea and sodium chloride ice at UHF and microwave frequencies," *J. Geophys. Res.*, 76, 4922–4931, July 1971 .

[18] M. R. Vant, R. B. Gray, R. O. Ramseier and V. Makios, " Dielectric properties of fresh and sea ice at 10 and 35 GHz," *J. Appl. Phys.*, 45, 4712–4717, Nov. 1974 .

[19] M. R. Vant, R. O. Ramseier and V. Makios, " The complex-dielectric constant of sea ice at frequencies in the range 0.1–40 GHz," *J. Appl. Phys.*, 49, 1264–1280, Mar. 1978 .

[20] W. F. Weeks and S. F. Ackley, " The growth, structure, and properties of sea ice," *CRREL Monograph 82-1*, USA Cold Regions Research and Engineering Laboratory, Hanover, NH, Nov. 1982 .

[21] R. M. Morey, A. Kovacs and G. F. N. Cox, " Electromagnetic properties of sea ice," *CRREL Monograph 84-2*, USA Cold Regions Research and Engineering Laboratory, Hanover, NH, Jan. 1984 .

[22] M. A. Zuniga and J. A. Kong and L. Tsang, " Depolarization effects in the active remote sensing of random media," *J. Appl. Phys.*, 51, 2315–2325, May 1980 .

[23] H. S. Tan, A. K. Fung and H. Eom, " A second-order renormalization theory for cross-polarized backscatter from a half space random medium," *Radio Science*, 15, 1059-1065, Nov.-Dec. 1980 .

[24] J. L. Powell and B. Crasemann, *Quantum Mechanics*, 272–274, Addison-Wesley Publishing Co., Inc., Reading, MA, 1961 .

[25] J. K. Lee and J. A. Kong, " Dyadic Green's functions for layered anisotropic medium," to be published in *Electromagnetics* .

[26] C. T. Tai, *Dyadic Green's Functions in Electromagnetic Theory*, 41–43, 57–65, Intex Educational Publishers, Scranton, PA, 1971 .

[27] C. M. Bender and S. A. Orszag, *Advanced Mathematical Methods for Scientists and Engineers*, 280–302, McGraw-Hill, Inc., New York, NY, 1978 .

[28] J. A. Kong, *Theory of Electromagnetic Waves*, 59–62, 205–212, John Wiley and Sons, Inc., NY, 1975 .

[29] A. Papoulis, *Probability, Random Variables and Stochastic Processes*, 336–384, McGraw-Hill, Inc., New York, NY, 1965 .

[30] F. Vallese and J. A. Kong, " Correlation function studies for snow and ice," *J. Appl. Phys.*, to be published .

[31] W. H. Peake, " Interaction of electromagnetic waves with some natural surfaces,"

IRE Trans., AP-7, S324-S329, 1959 .

[32] J. K. Lee, " Active microwave remote sensing of a two-layer anisotropic random medium," *S.M. Thesis*, MIT, Cambridge, MA, May 1981 .

[33] M. C. Kubacsi, " Radiative transfer theory for remote sensing of layered homogeneous media containing ellipsoidal scatterers," *S. M. Thesis*, MIT, Cambridge, MA, May 1981 .

Figure Captions

Figure 1 Scattering geometry of a two-layer anisotropic random medium..

Figure 2 Geometrical configuration of permittivity tensor..

Figure 3 Theoretical results of σ_{HH}, σ_{VV} and σ_{HV} versus incidence angle ($\theta_{oi} = 30°$, $\phi_{oi} = 0°$ ..

Figure 4 Theoretical results of σ_{HH} and σ_{VV} versus incidence angle (θ_{oi} at f = 10 GHz, $\phi_{oi} = 0°$ ..

Figure 5 Theoretical results of σ_{HH} and σ_{VV} versus inciddence angle with $\phi_{oi} = 80°$ when $\delta_1 > \delta_2$ ..

Figure 6 Theoretical results of σ_{HH} and σ_{VV} versus incidence angle with $\phi_{oi} =$ 10° when $\delta_1 < \delta_2$ ..

Figure 7 Theoretical results of σ_{HH} and σ_{VV} versus incidence angle with $\phi_{oi} =$ 10° when $\delta_1 < \delta_2$ ..

Figure 8 Effect of anisotropic background on incidence angle response..

Figure 9 Theoretical results of σ_{HH}, σ_{VV} and σ_{HV} versus incidence azimuthal angle (ϕ_{oi}) at $\theta_{oi} = 30°$ when $\delta_1 > \delta_2$ ..

Figure 10 Theoretical results of σ_{HH}, σ_{VV} and σ_{HV} versus incidence azimuthal angle at $\theta_{oi} = 10°$ when $\delta_1 < \delta_2$ ..

Figure 11 Theoretical results of σ_{HH}, σ_{VV} and σ_{HV} versus tilted angle ($\psi = \psi_f$)

at $\theta_{oi} = 30°$, $\phi_{oi} = 10°$ ..

Figure 12 Theoretical results of σ_{HH}, σ_{VV} and σ_{HV} versus tilted angle (ψ_f) with $\psi = 0°$ at $\theta_{oi} = 30°$, $\phi_{oi} = 10°$ ..

Figure 13 Interpretation of backscattering data of thick first-year sea ice as a function of incidence angle at f = 9 GHz..

Figure 14 Interpretation of backscattering data of the same sea ice at f = 13 GHz..

Figure 15 Interpretation of backscattering data of the same sea ice at f = 17 GHz..

Figure 16 Interpretation of backscattering data of multiyear sea ice as a function of incidence angle at f = 9 GHz..

Figure 17 Interpretation of backscattering data of the same sea ice at f = 13 GHz..

Figure 18 Interpretation of backscattering data of the same sea ice at f = 17 GHz..

Figure 1

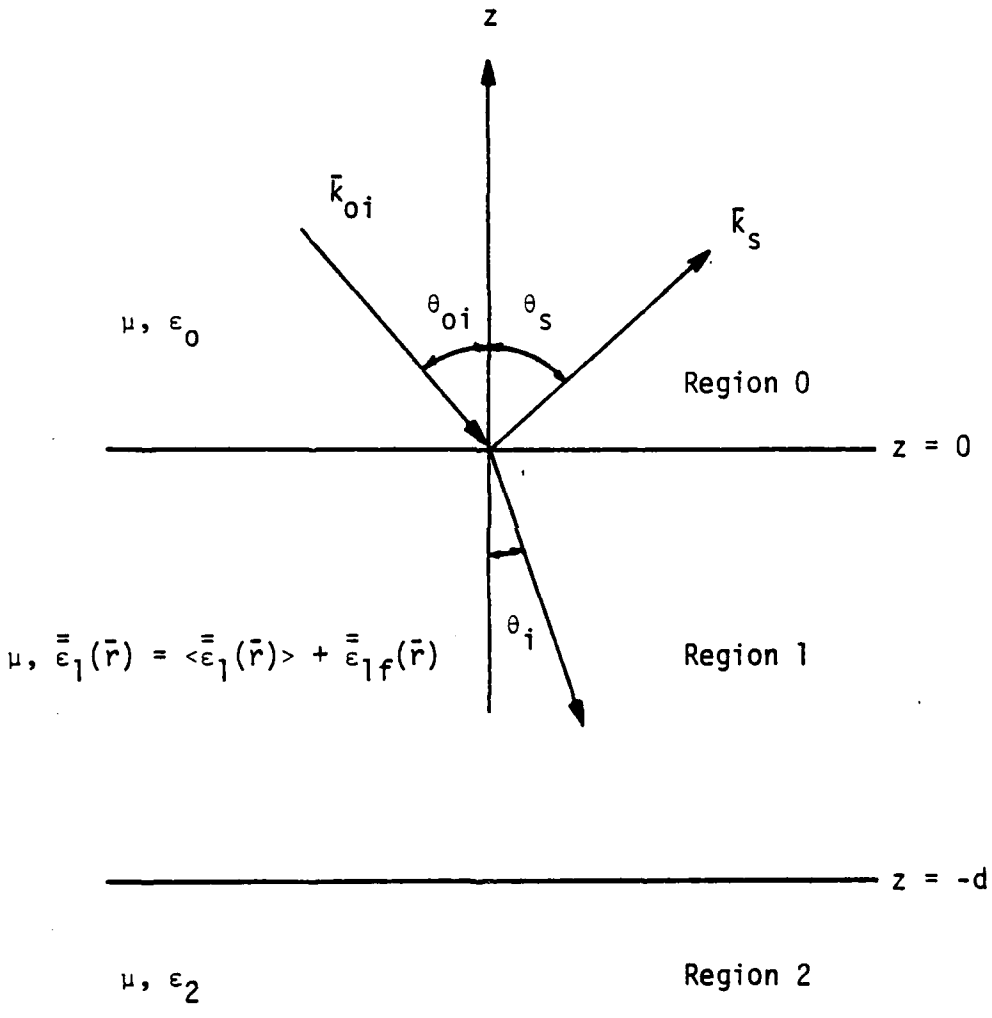
z
$\bar{k}_{oi}$
$\bar{k}_s$
θ_{oi}
θ_s
μ, ε_o
Region 0
z = 0
θ_i
$\mu, \bar{\bar{\varepsilon}}_1(\bar{r}) = \langle\bar{\bar{\varepsilon}}_1(\bar{r})\rangle + \bar{\bar{\varepsilon}}_{1f}(\bar{r})$
Region 1
z = -d
μ, ε_2
Region 2

Figure 2

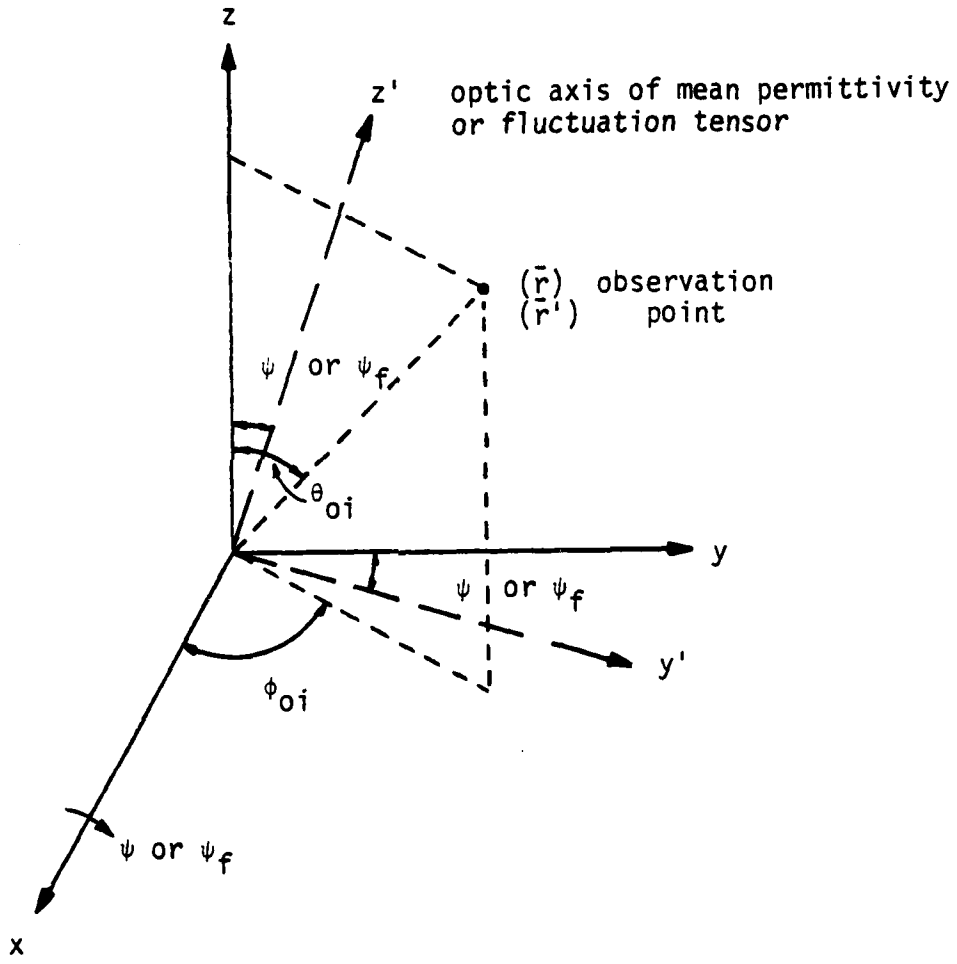
z
z'
optic axis of mean permittivity
or fluctuation tensor
$(\bar{r})$ observation
$(\bar{r}')$ point
ψ or ψ_f
θ_{oi}
y
ψ or ψ_f
y'
ϕ_{oi}
ψ or ψ_f
x

Figure 3

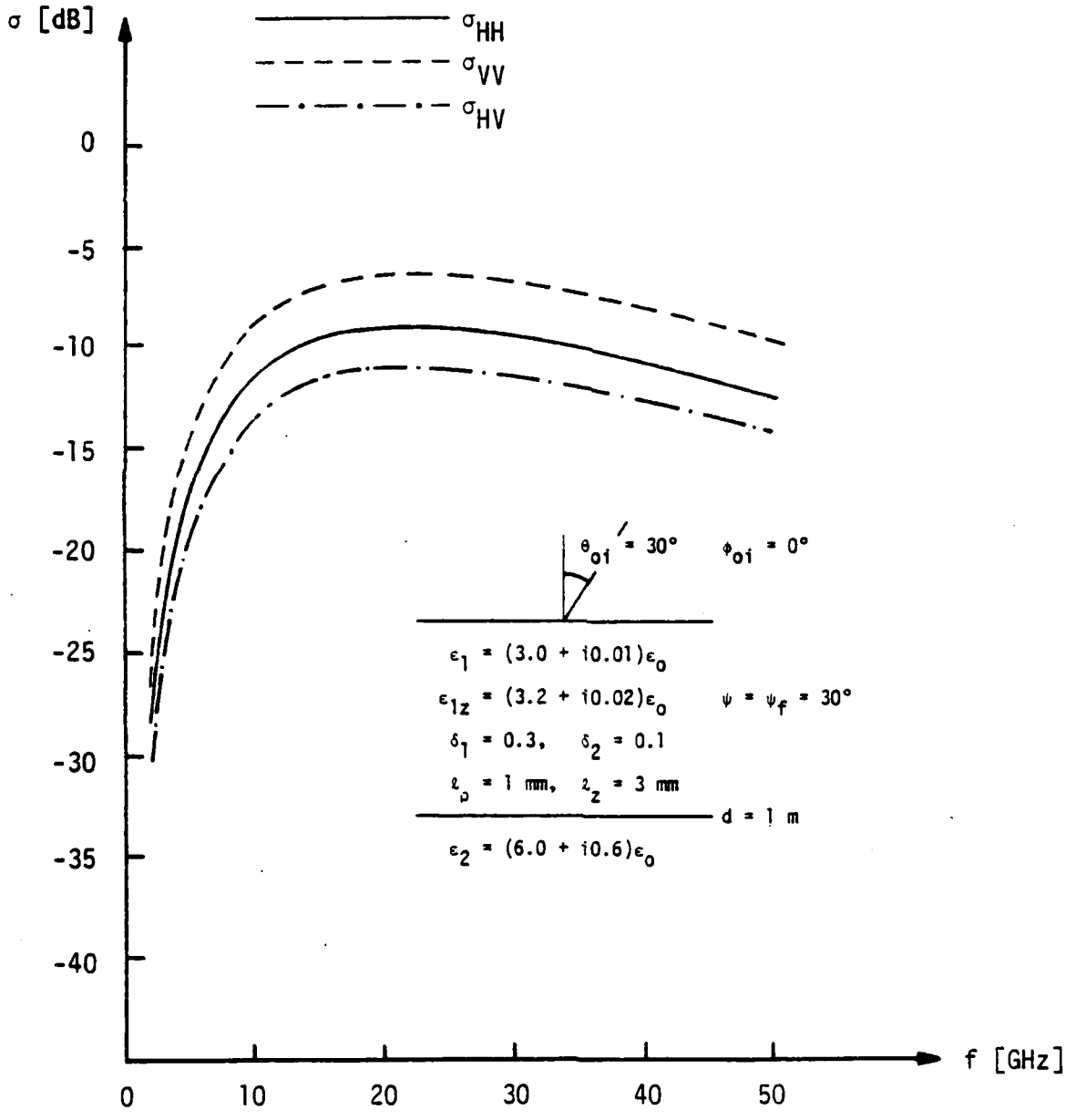
σ [dB]
σHH
σVV
σHV
0
-5
-10
-15
-20
-25
-30
-35
-40
0
10
20
30
40
50
f [GHz]
θoi = 30°
φoi = 0°
ε1 = (3.0 + i0.01)ε0
ε1z = (3.2 + i0.02)ε0
ψ = ψf = 30°
δ1 = 0.3, δ2 = 0.1
ℓρ = 1 mm, ℓz = 3 mm
d = 1 m
ε2 = (6.0 + i0.6)ε0

Figure 4

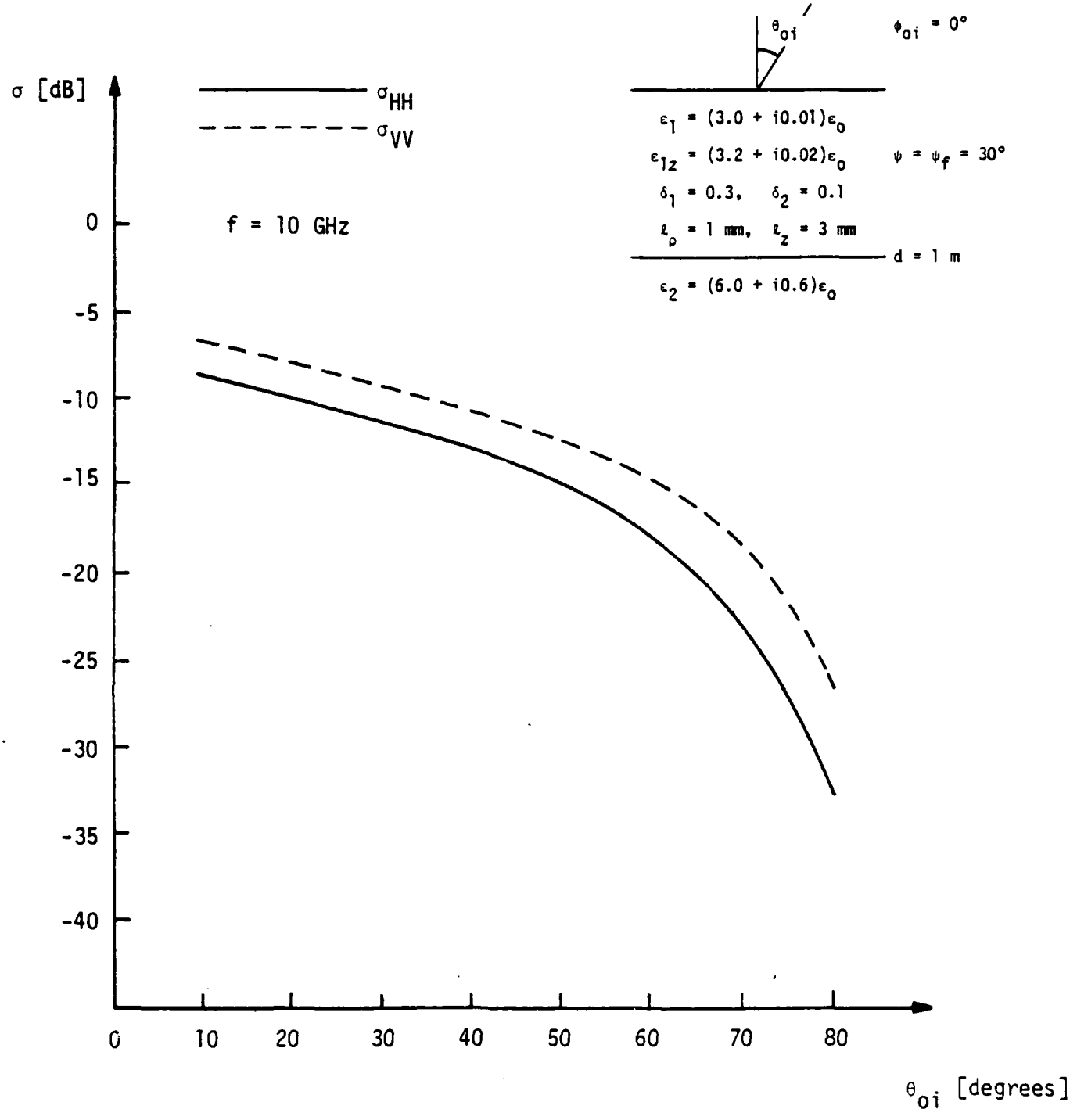
σ [dB]
σHH
σVV
f = 10 GHz
θoi
φoi = 0°
ε1 = (3.0 + i0.01)ε0
ε1z = (3.2 + i0.02)ε0
ψ = ψf = 30°
δ1 = 0.3, δ2 = 0.1
ℓρ = 1 mm, ℓz = 3 mm
d = 1 m
ε2 = (6.0 + i0.6)ε0
0
-5
-10
-15
-20
-25
-30
-35
-40
0
10
20
30
40
50
60
70
80
θoi [degrees]

Figure 5

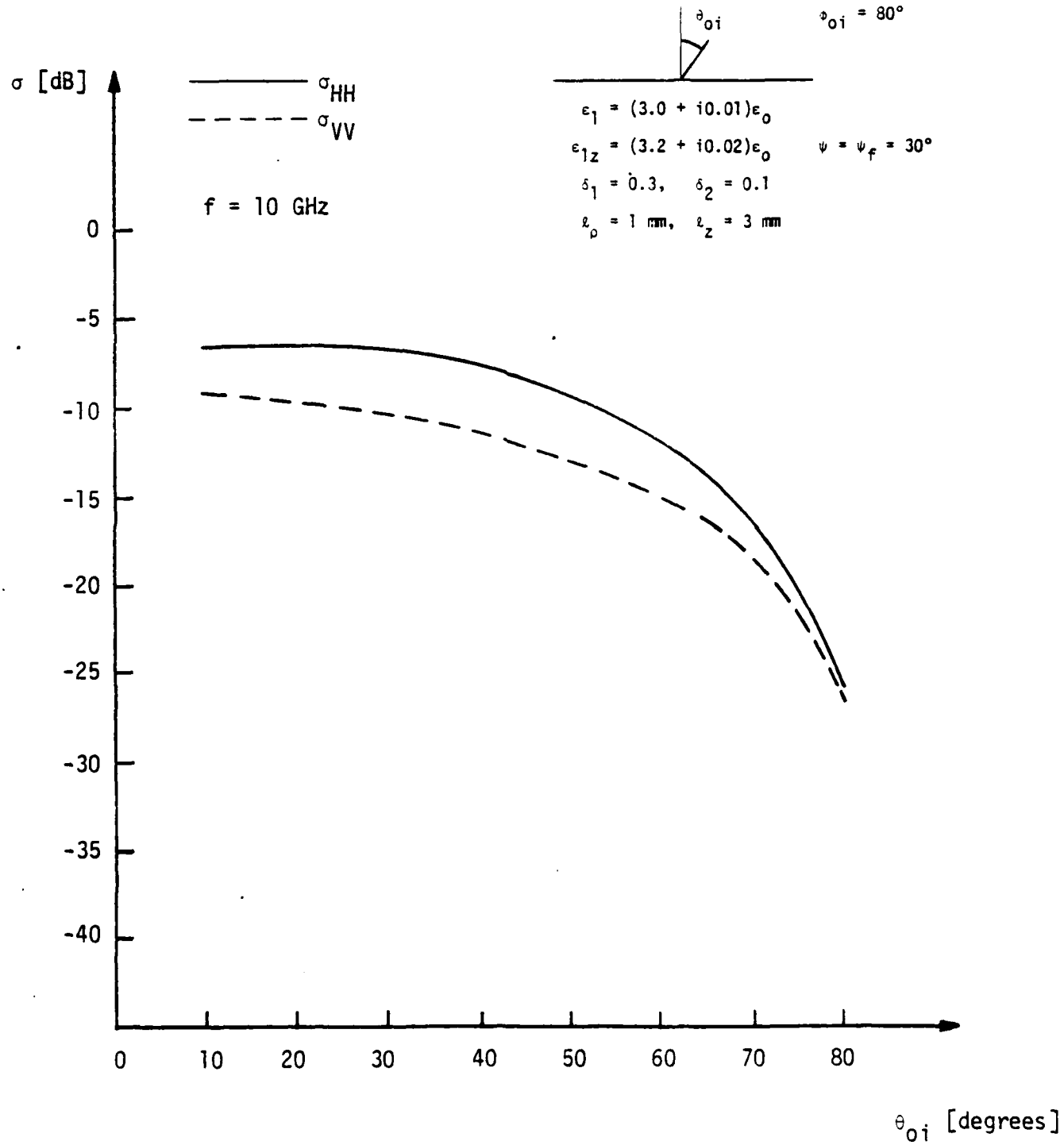
σ [dB]
σHH
σVV
f = 10 GHz
ϑoi
φoi = 80°
ε1 = (3.0 + i0.01)ε0
ε1z = (3.2 + i0.02)ε0
ψ = ψf = 30°
δ1 = 0.3, δ2 = 0.1
ℓρ = 1 mm, ℓz = 3 mm
0
-5
-10
-15
-20
-25
-30
-35
-40
0
10
20
30
40
50
60
70
80
θoi [degrees]

Figure 6

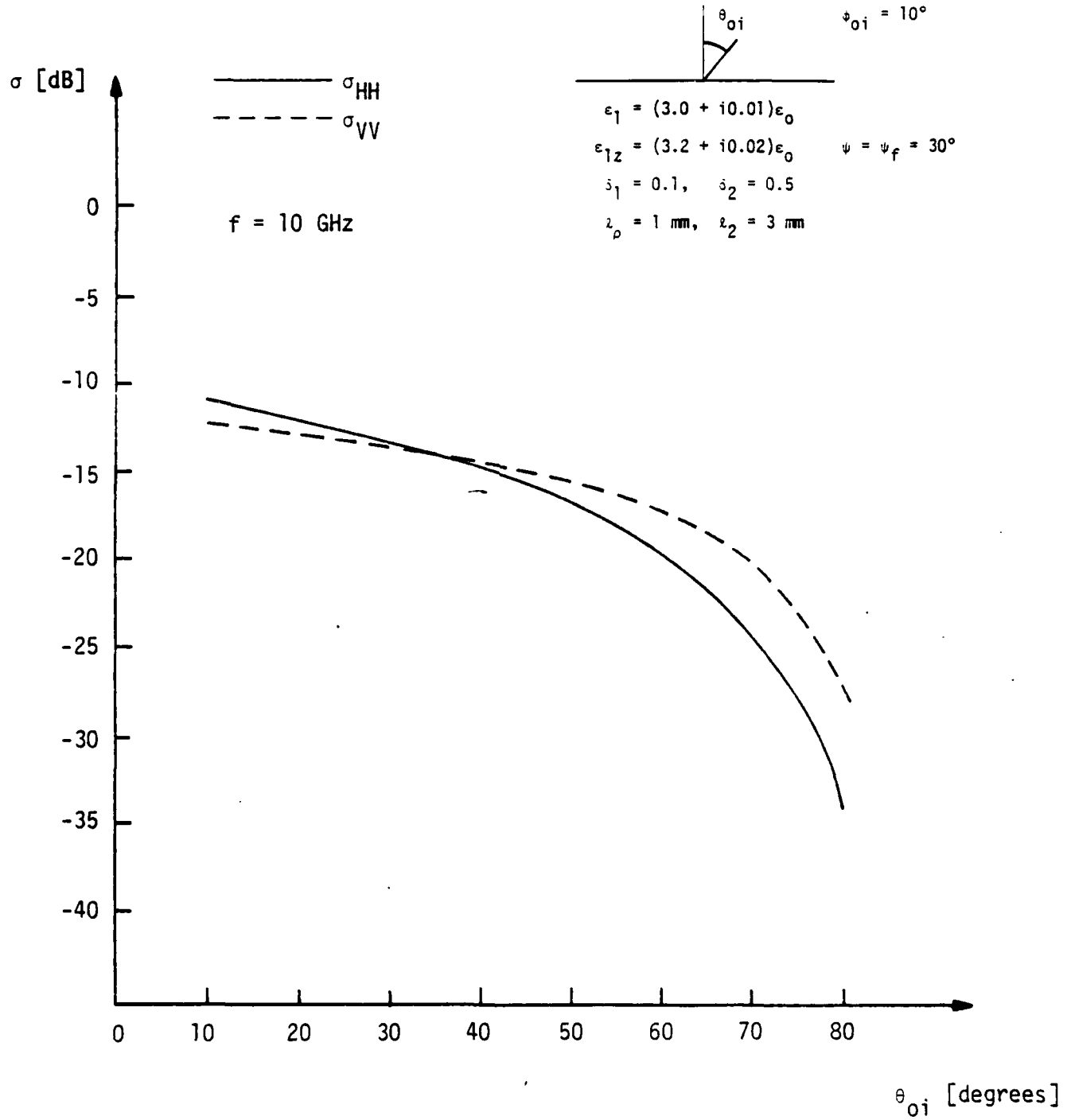
θ_{oi}
$\phi_{oi} = 10°$
σ [dB]
σ_{HH}
σ_{VV}
$\varepsilon_1 = (3.0 + i0.01)\varepsilon_o$
$\varepsilon_{1z} = (3.2 + i0.02)\varepsilon_o$
$\psi = \psi_f = 30°$
$\delta_1 = 0.1, \quad \delta_2 = 0.5$
$\ell_\rho = 1$ mm, $\ell_2 = 3$ mm
f = 10 GHz
0
-5
-10
-15
-20
-25
-30
-35
-40
0
10
20
30
40
50
60
70
80
θ_{oi} [degrees]

Figure 7

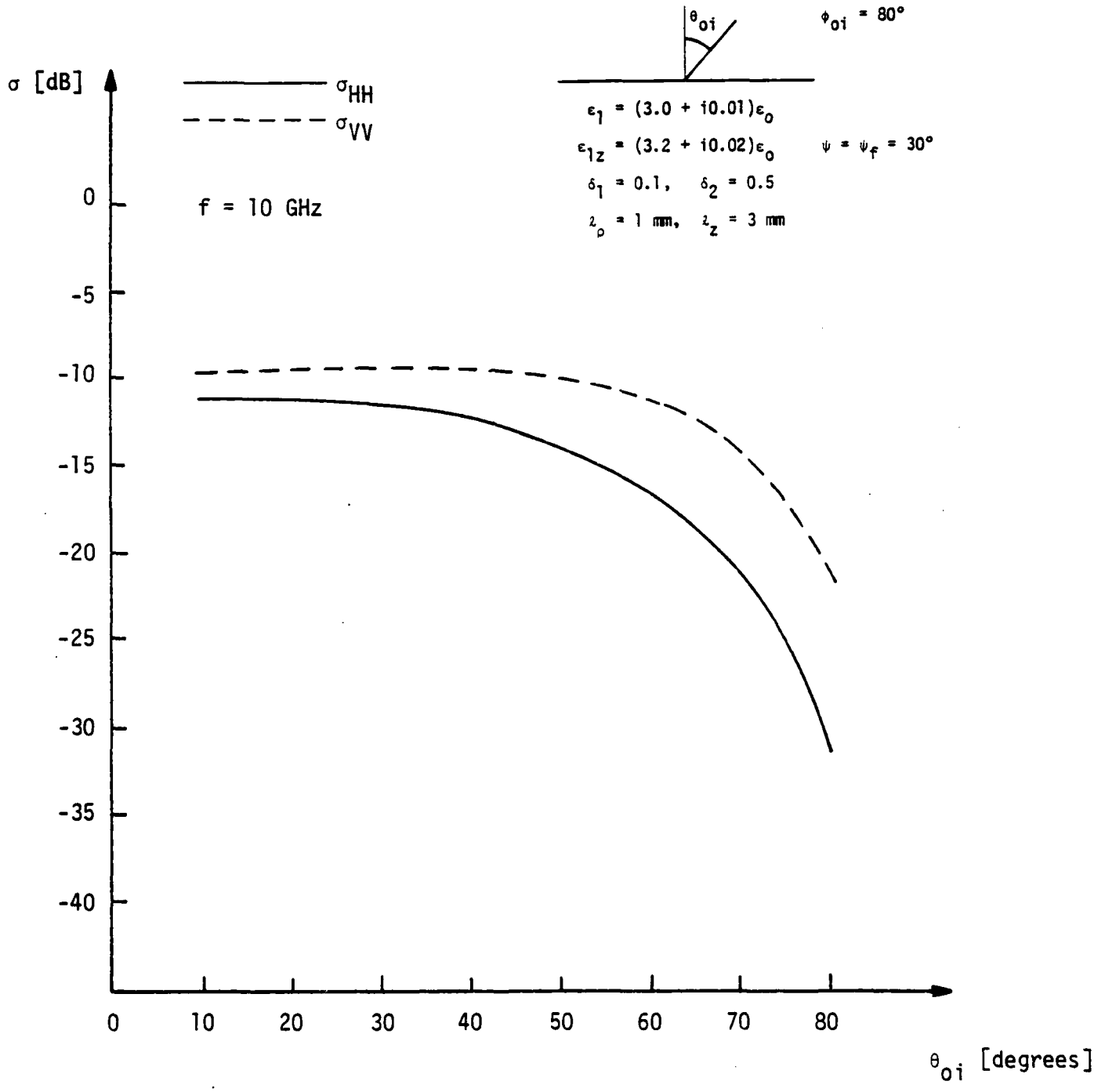
θ_{oi}
$\phi_{oi} = 80°$
σ [dB]
σ_{HH}
σ_{VV}
$\epsilon_1 = (3.0 + i0.01)\epsilon_o$
$\epsilon_{1z} = (3.2 + i0.02)\epsilon_o$
$\psi = \psi_f = 30°$
$\delta_1 = 0.1, \quad \delta_2 = 0.5$
$\ell_\rho = 1$ mm, $\ell_z = 3$ mm
f = 10 GHz
0
-5
-10
-15
-20
-25
-30
-35
-40
0
10
20
30
40
50
60
70
80
θ_{oi} [degrees]

Figure 8

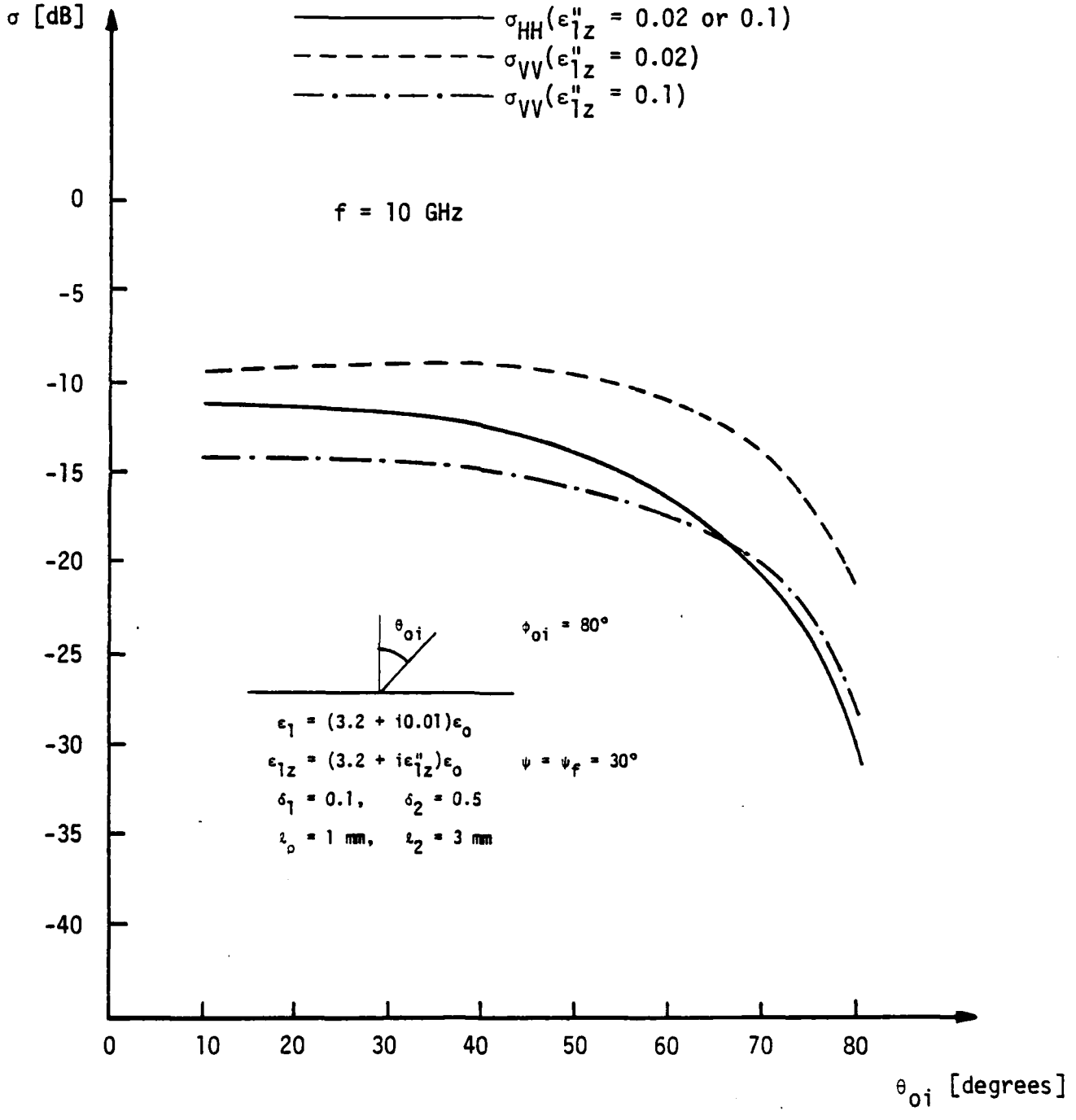
σ [dB]
$\sigma_{HH}(\varepsilon''_{1z} = 0.02 \text{ or } 0.1)$
$\sigma_{VV}(\varepsilon''_{1z} = 0.02)$
$\sigma_{VV}(\varepsilon''_{1z} = 0.1)$
f = 10 GHz
0
-5
-10
-15
-20
-25
-30
-35
-40
θ_{oi}
$\phi_{oi} = 80°$
$\varepsilon_1 = (3.2 + i0.01)\varepsilon_o$
$\varepsilon_{1z} = (3.2 + i\varepsilon''_{1z})\varepsilon_o$
$\psi = \psi_f = 30°$
$\delta_1 = 0.1, \quad \delta_2 = 0.5$
$\ell_o = 1$ mm, $\ell_2 = 3$ mm
0
10
20
30
40
50
60
70
80
θ_{oi} [degrees]

Figure 9

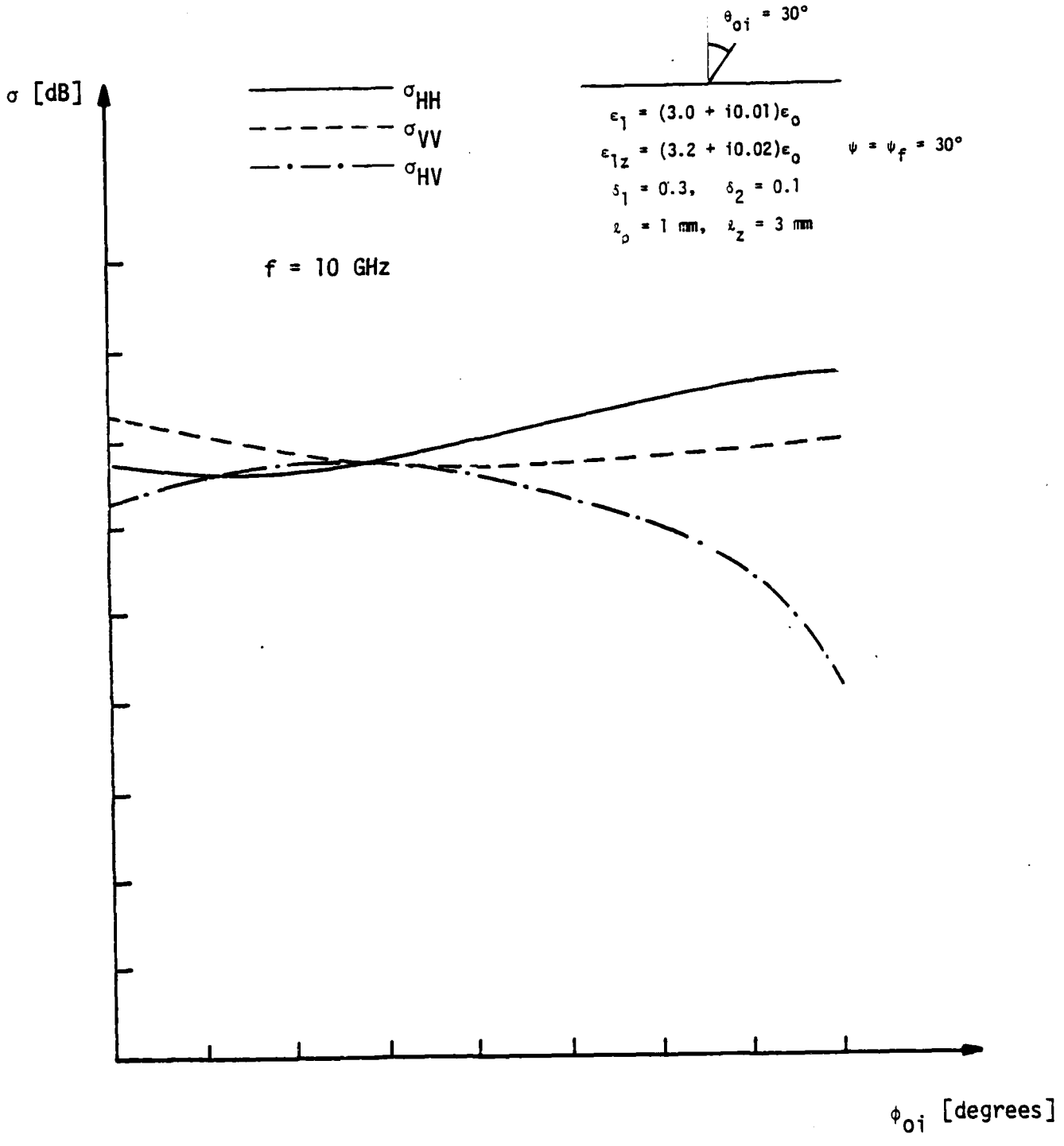
θ_{oi} = 30°
σ [dB]
σ_{HH}
σ_{VV}
σ_{HV}
$\epsilon_1 = (3.0 + i0.01)\epsilon_o$
$\epsilon_{1z} = (3.2 + i0.02)\epsilon_o$
$\psi = \psi_f$ = 30°
δ_1 = 0.3, δ_2 = 0.1
ℓ_ρ = 1 mm, ℓ_z = 3 mm
f = 10 GHz
ϕ_{oi} [degrees]

Figure 10

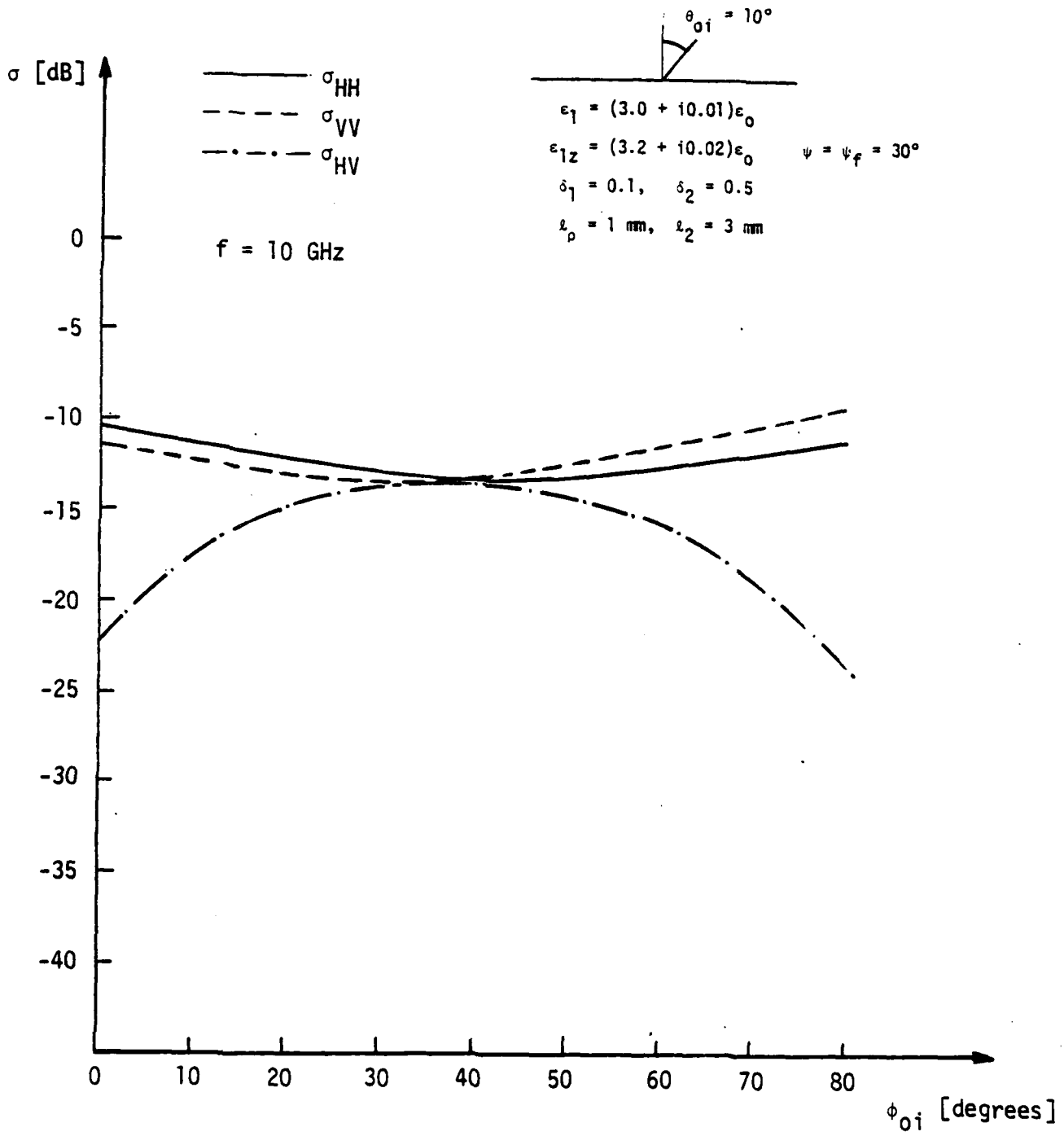
σ [dB]
σHH
σVV
σHV
f = 10 GHz
θoi = 10°
ε1 = (3.0 + i0.01)ε0
ε1z = (3.2 + i0.02)ε0
ψ = ψf = 30°
δ1 = 0.1, δ2 = 0.5
ℓρ = 1 mm, ℓ2 = 3 mm
0
-5
-10
-15
-20
-25
-30
-35
-40
0
10
20
30
40
50
60
70
80
φoi [degrees]

Figure 11

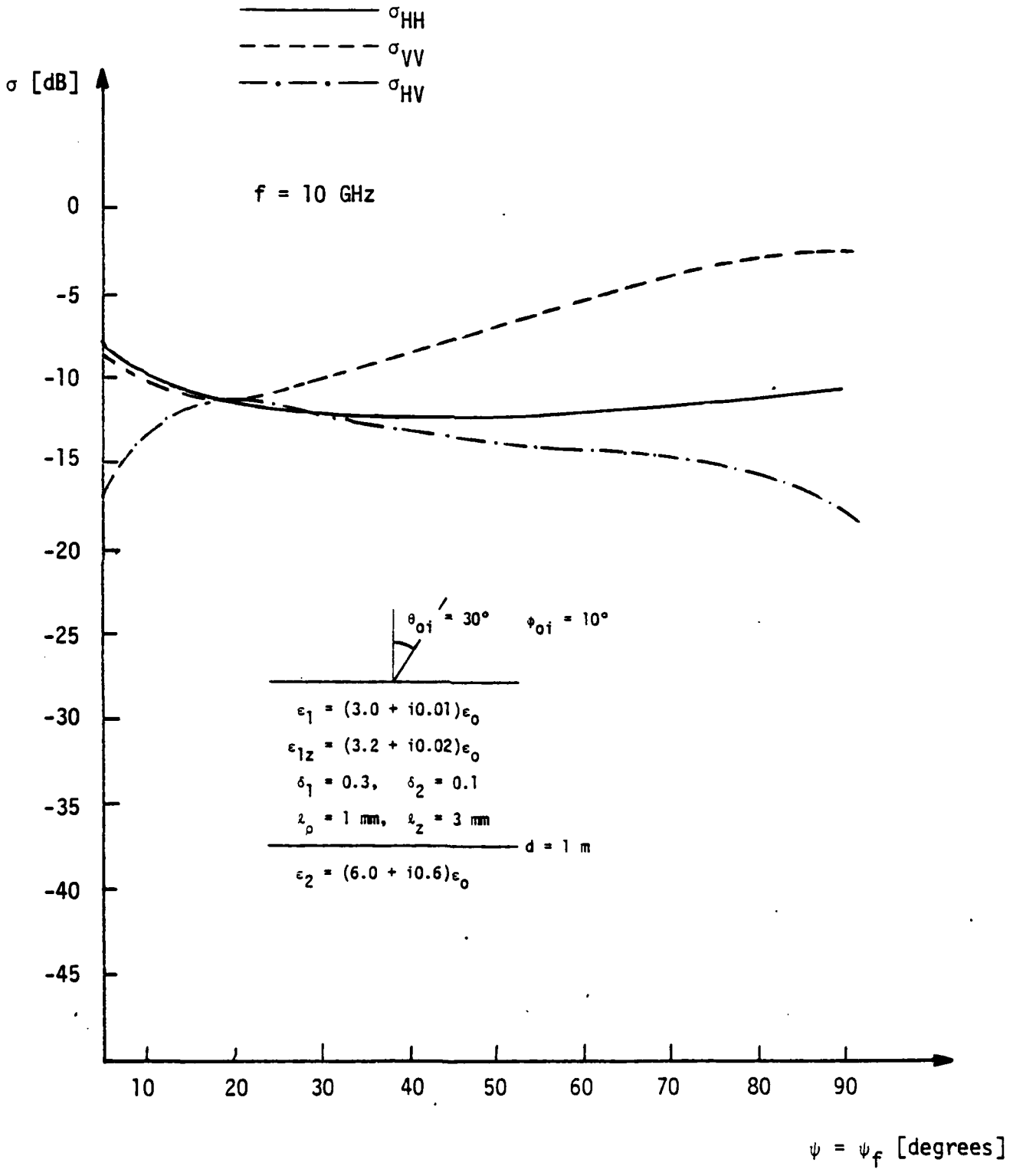
σ_{HH}
σ_{VV}
σ_{HV}
σ [dB]
f = 10 GHz
0
-5
-10
-15
-20
-25
-30
-35
-40
-45
10
20
30
40
50
60
70
80
90
$\psi = \psi_f$ [degrees]
$\theta_{oi} = 30°$
$\phi_{oi} = 10°$
$\varepsilon_1 = (3.0 + i0.01)\varepsilon_o$
$\varepsilon_{1z} = (3.2 + i0.02)\varepsilon_o$
$\delta_1 = 0.3, \quad \delta_2 = 0.1$
$\ell_\rho = 1$ mm, $\ell_z = 3$ mm
d = 1 m
$\varepsilon_2 = (6.0 + i0.6)\varepsilon_o$

Figure 12

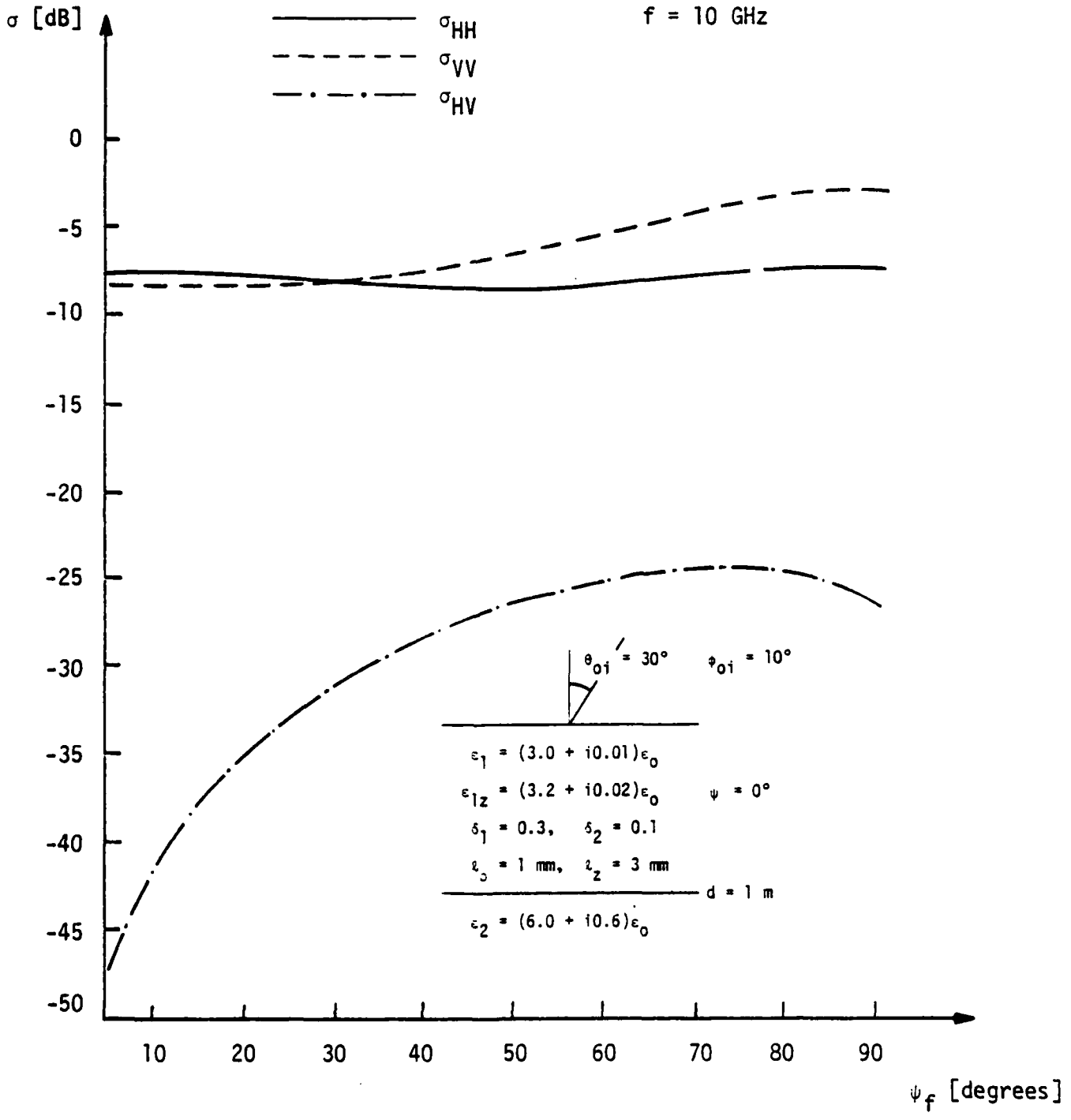
σ [dB]
σHH
σVV
σHV
f = 10 GHz
0
-5
-10
-15
-20
-25
-30
-35
-40
-45
-50
θoi = 30°
φoi = 10°
ε1 = (3.0 + i0.01)ε0
ε1z = (3.2 + i0.02)ε0
ψ = 0°
δ1 = 0.3, δ2 = 0.1
ℓx = 1 mm, ℓz = 3 mm
d = 1 m
ε2 = (6.0 + i0.6)ε0
10
20
30
40
50
60
70
80
90
ψf [degrees]

Figure 13

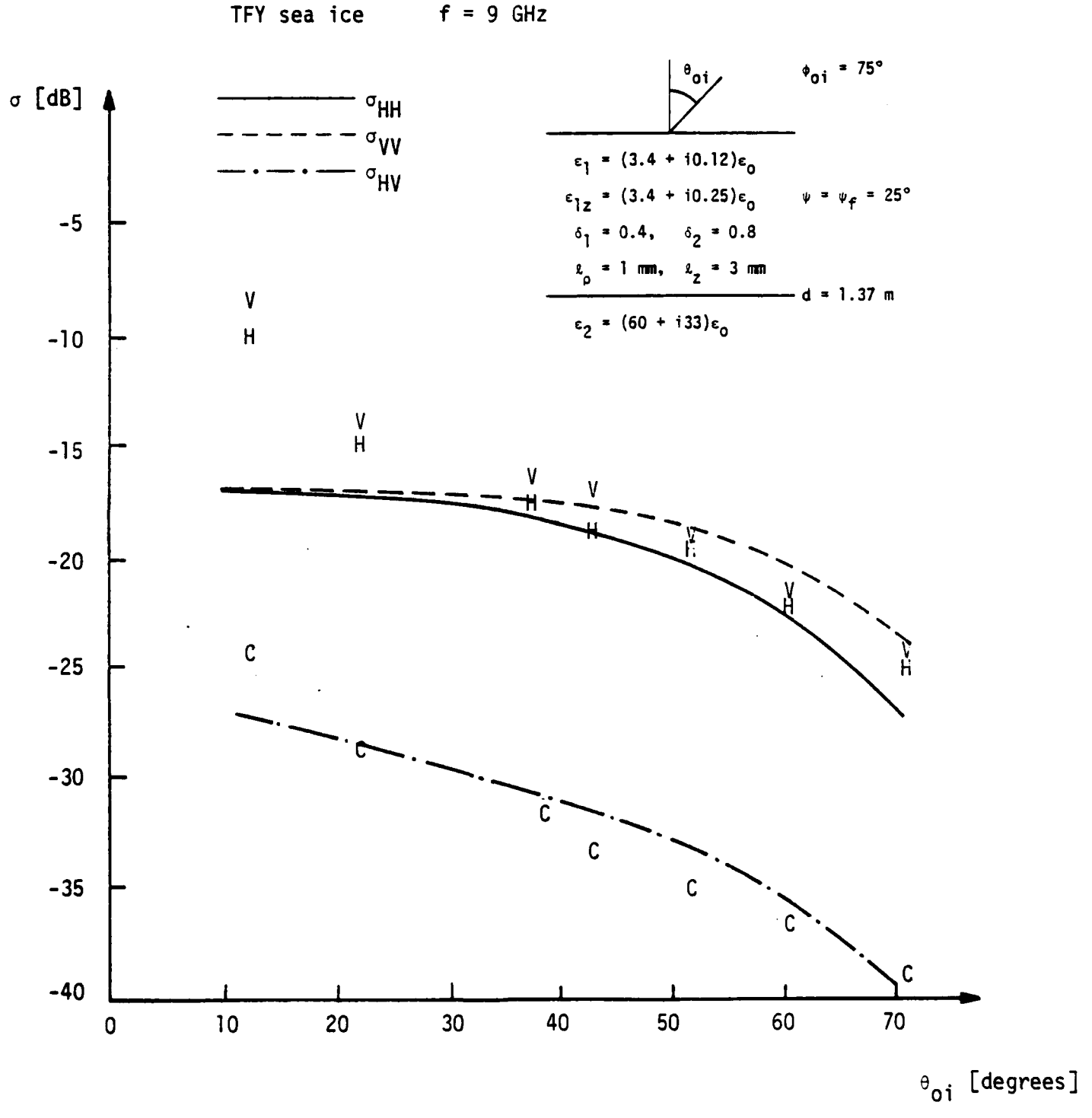
TFY sea ice
f = 9 GHz
σ [dB]
σ_{HH}
σ_{VV}
σ_{HV}
θ_{oi}
ϕ_{oi} = 75°
$\varepsilon_1 = (3.4 + i0.12)\varepsilon_o$
$\varepsilon_{1z} = (3.4 + i0.25)\varepsilon_o$
$\psi = \psi_f = 25°$
$\delta_1 = 0.4, \quad \delta_2 = 0.8$
ℓ_ρ = 1 mm, ℓ_z = 3 mm
d = 1.37 m
$\varepsilon_2 = (60 + i33)\varepsilon_o$
-5
-10
-15
-20
-25
-30
-35
-40
0
10
20
30
40
50
60
70
θ_{oi} [degrees]

Figure 14

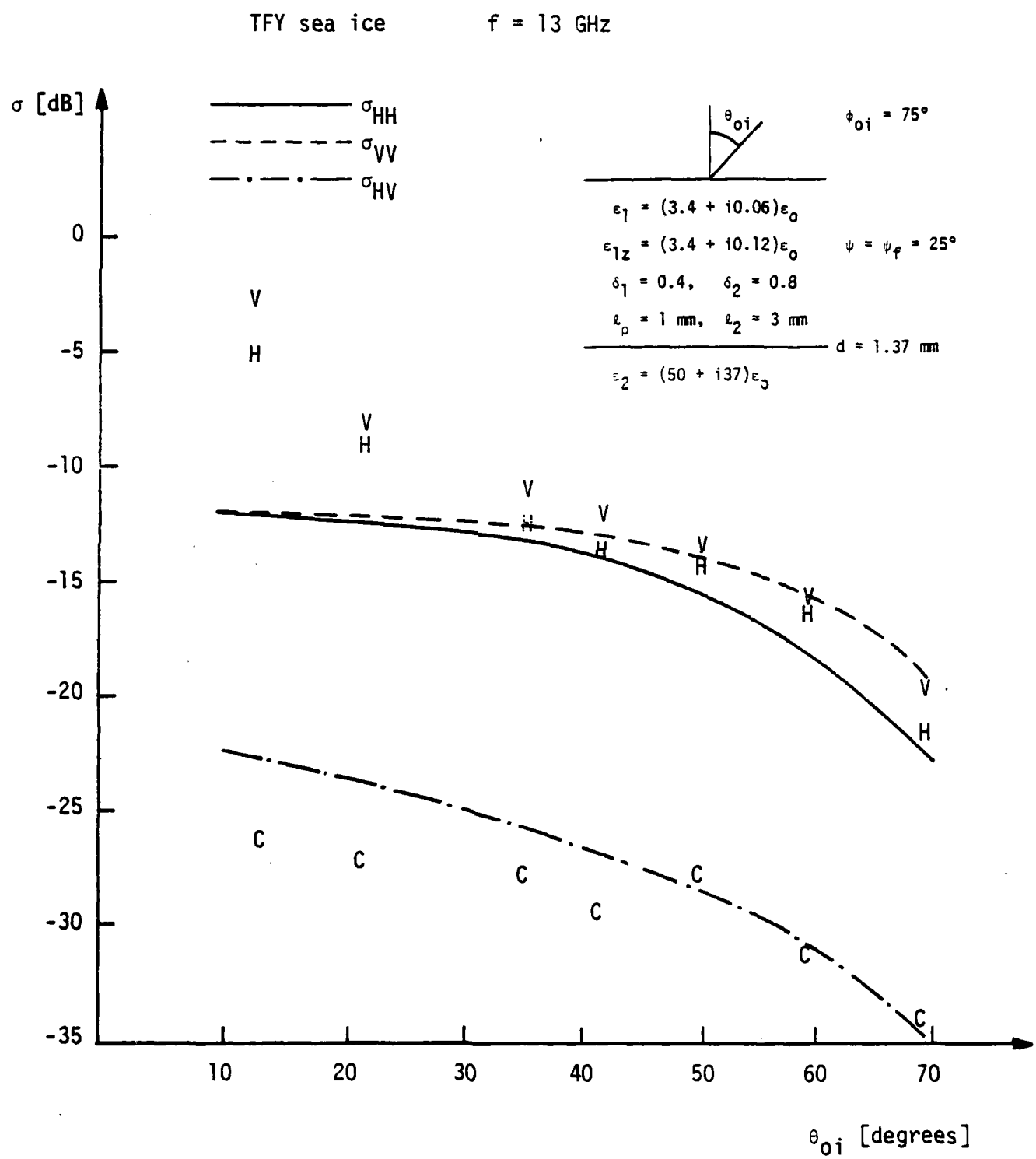
TFY sea ice
f = 13 GHz
σ [dB]
σHH
σVV
σHV
θoi
φoi = 75°
ε1 = (3.4 + i0.06)ε0
ε1z = (3.4 + i0.12)ε0
ψ = ψf = 25°
δ1 = 0.4, δ2 = 0.8
ℓp = 1 mm, ℓ2 = 3 mm
d = 1.37 mm
ε2 = (50 + i37)ε0
0
-5
-10
-15
-20
-25
-30
-35
10
20
30
40
50
60
70
θoi [degrees]

Figure 15

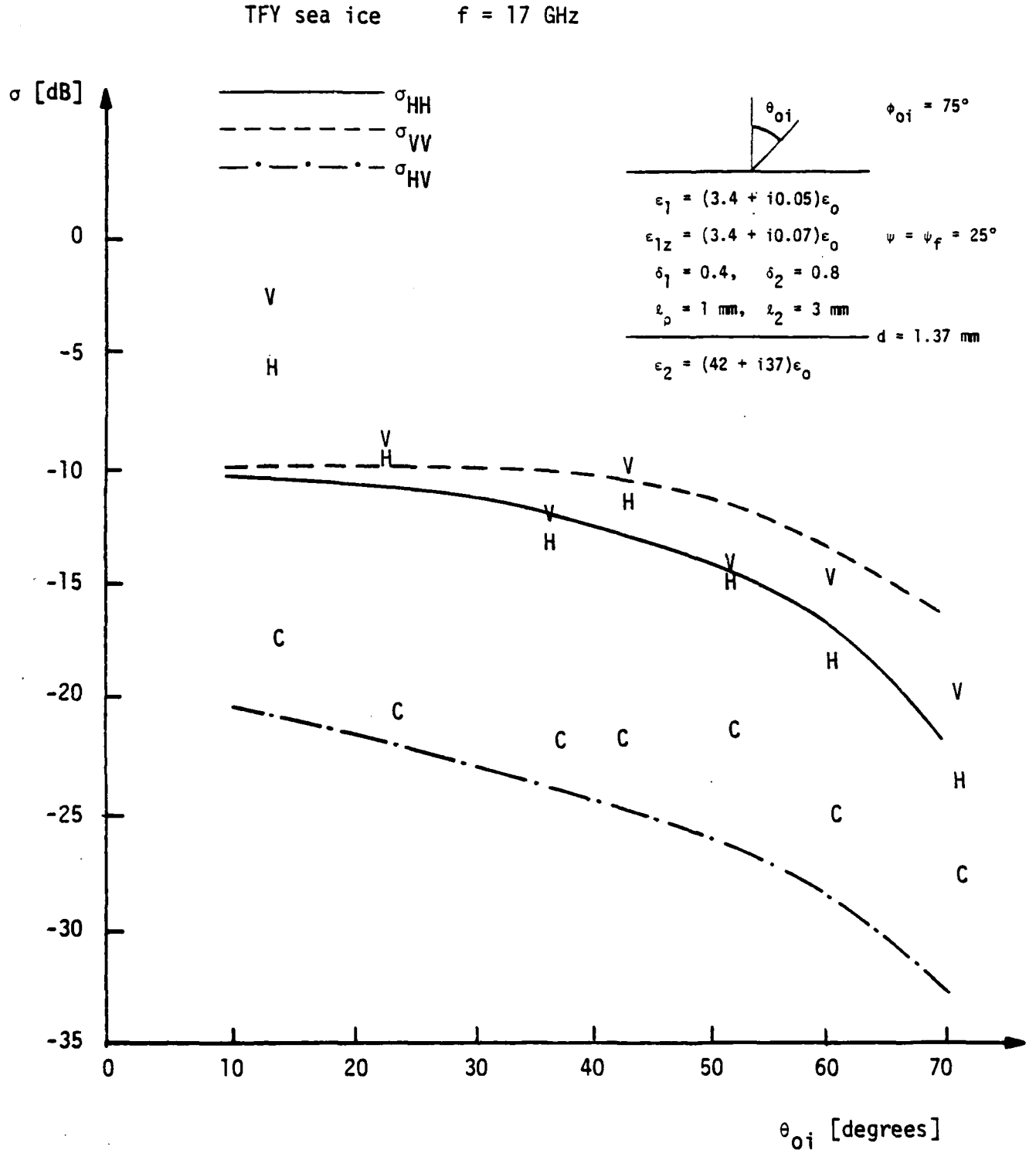
TFY sea ice f = 17 GHz
σ [dB]
σ_{HH}
σ_{VV}
σ_{HV}
θ_{oi}
ϕ_{oi} = 75°
$\varepsilon_1 = (3.4 + i0.05)\varepsilon_o$
$\varepsilon_{1z} = (3.4 + i0.07)\varepsilon_o$
$\psi = \psi_f$ = 25°
δ_1 = 0.4, δ_2 = 0.8
ℓ_ρ = 1 mm, ℓ_2 = 3 mm
d = 1.37 mm
$\varepsilon_2 = (42 + i37)\varepsilon_o$
0
-5
-10
-15
-20
-25
-30
-35
0
10
20
30
40
50
60
70
θ_{oi} [degrees]

Figure 16

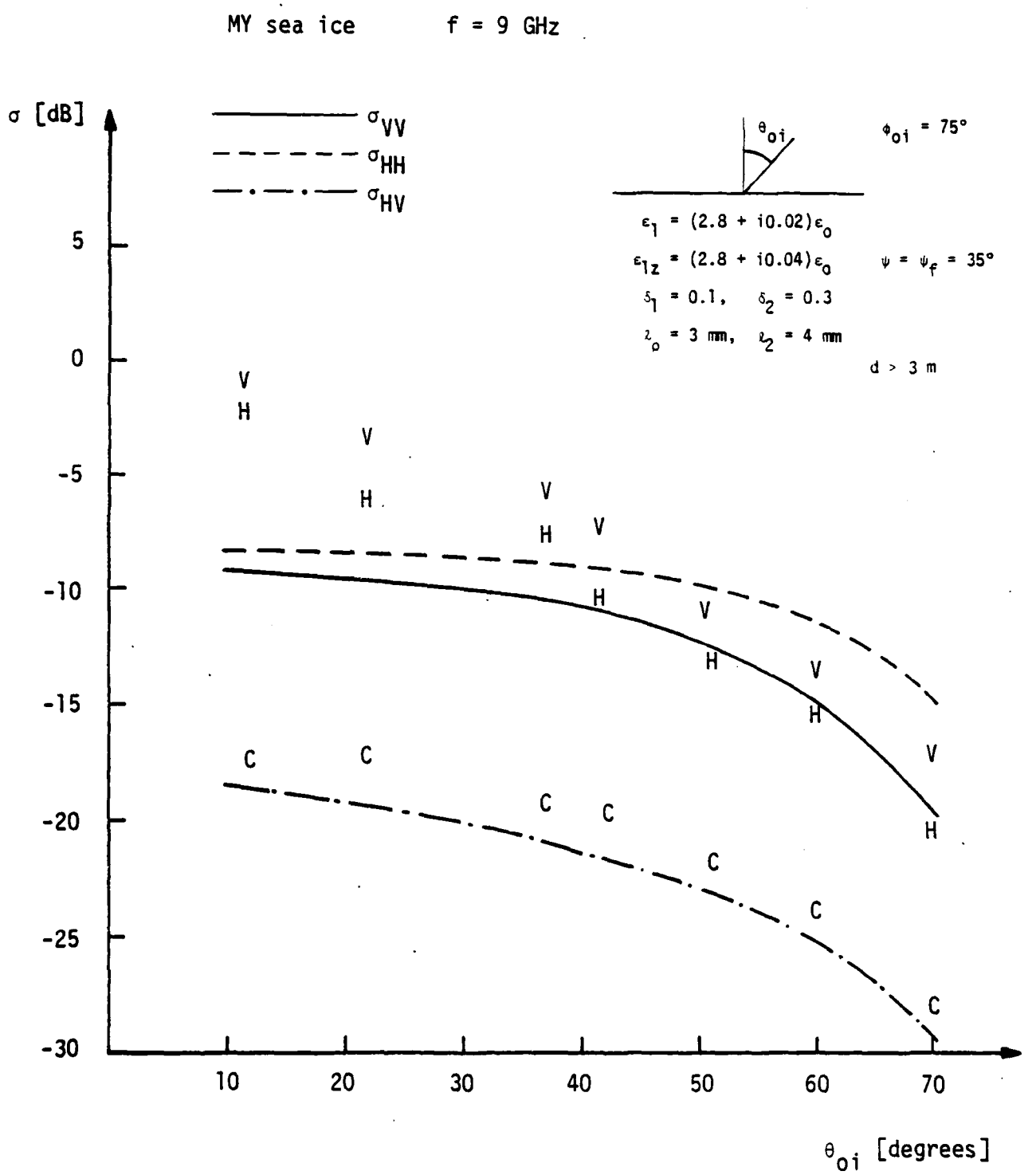
MY sea ice
f = 9 GHz
σ [dB]
σVV
σHH
σHV
θoi
φoi = 75°
ε1 = (2.8 + i0.02)ε0
ε1z = (2.8 + i0.04)ε0
ψ = ψf = 35°
δ1 = 0.1, δ2 = 0.3
ℓ0 = 3 mm, ℓ2 = 4 mm
d > 3 m
5
0
-5
-10
-15
-20
-25
-30
10
20
30
40
50
60
70
θoi [degrees]

Figure 17

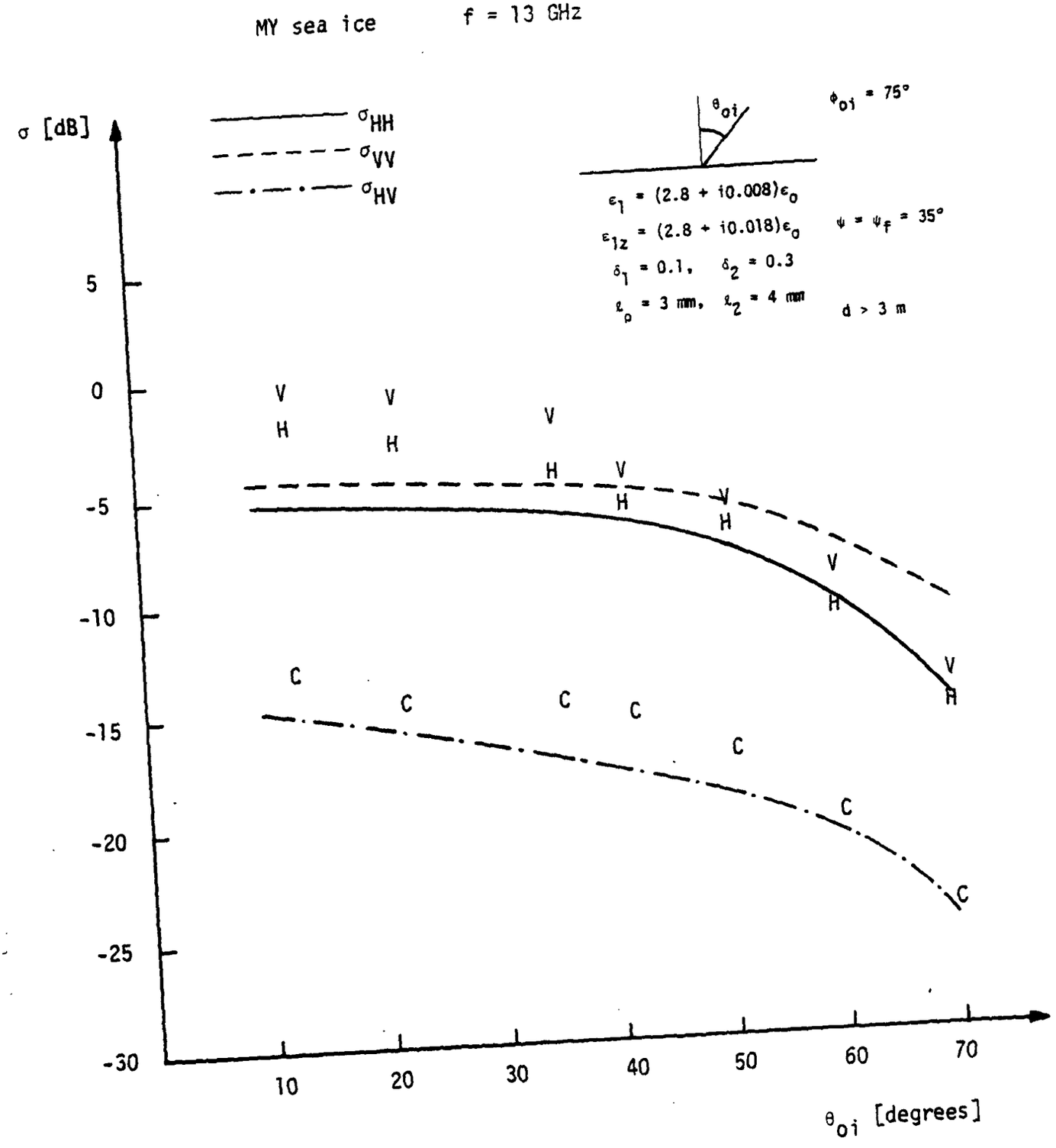
MY sea ice
f = 13 GHz
σ [dB]
σ_{HH}
σ_{VV}
σ_{HV}
θ_{oi}
ϕ_{oi} = 75°
$\epsilon_1 = (2.8 + i0.008)\epsilon_o$
$\epsilon_{1z} = (2.8 + i0.018)\epsilon_o$
$\psi = \psi_f = 35°$
$\delta_1 = 0.1$, $\delta_2 = 0.3$
$\ell_p = 3$ mm, $\ell_2 = 4$ mm
d > 3 m
5
0
-5
-10
-15
-20
-25
-30
10
20
30
40
50
60
70
θ_{oi} [degrees]

Figure 18

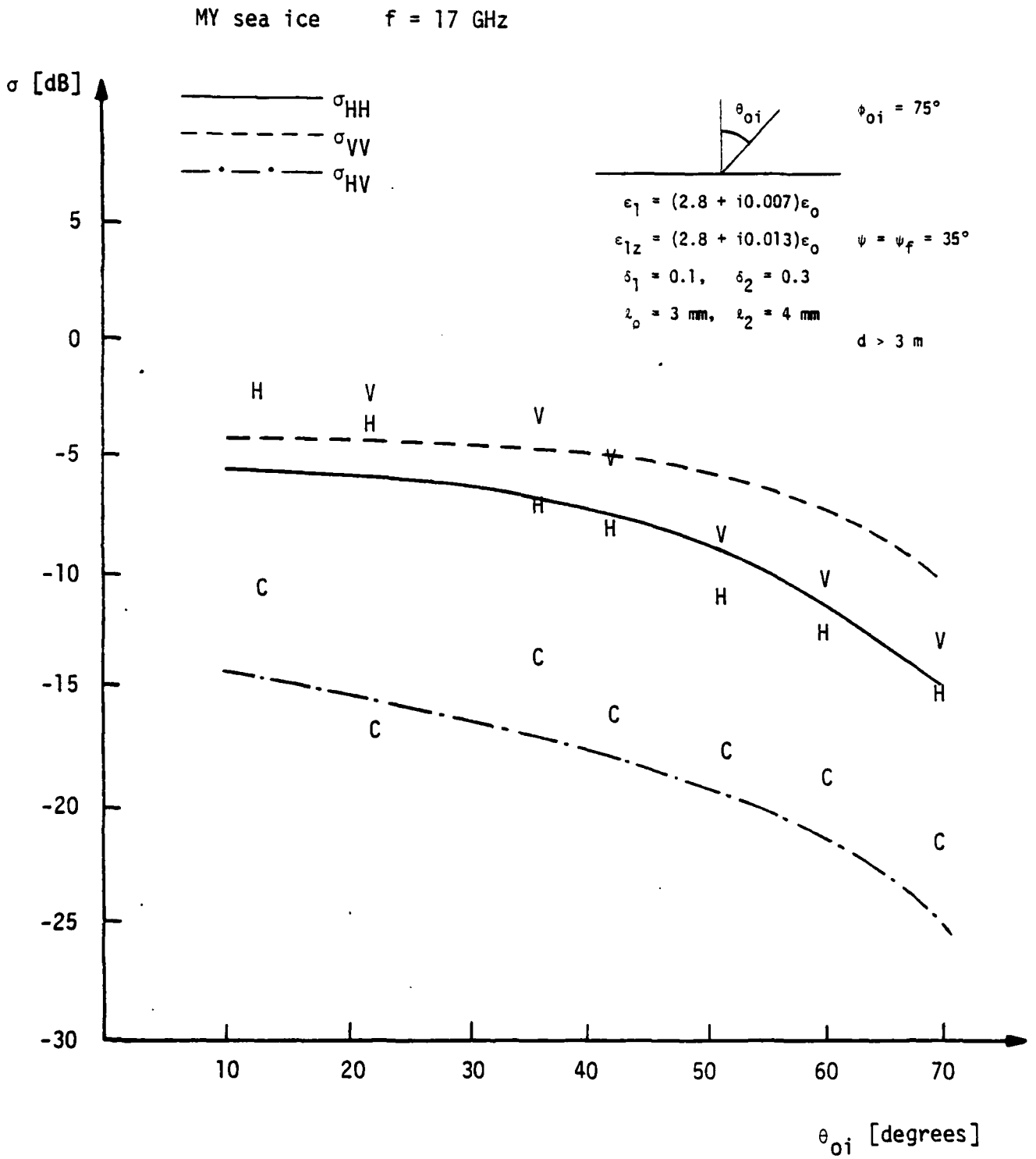
MY sea ice f = 17 GHz
σ [dB]
σHH
σVV
σHV
θoi
φoi = 75°
ε1 = (2.8 + i0.007)ε0
ε1z = (2.8 + i0.013)ε0
ψ = ψf = 35°
δ1 = 0.1, δ2 = 0.3
ℓ0 = 3 mm, ℓ2 = 4 mm
d > 3 m
5
0
-5
-10
-15
-20
-25
-30
10
20
30
40
50
60
70
θoi [degrees]

DISTRIBUTION LIST

	DODAAD Code	
Leader, Artic, Atmospheric and Ionospheric Sciences Division Office of Naval Research 800 North Quincy Street Arlington, Virginia 22217	N00014	(1)
Administrative Contracting Officer ONRRR - E19-628 Massachusetts Institute of Technology Cambridge, Massachusetts 02139	N66017	(1)
Director Naval Research Laboratory Attn: Code 2627 Washington, D.C. 20375	N00173	(6)
Defense Technical Information Center Bldg. 5, Cameron Station Alexandria, Virginia 22314	S47031	(12)

END

FILMED

DTIC